ELSEVIER

International Journal of Solids and Structures 41 (2004) 5383–5409

INTERNATIONAL JOURNAL OF SOLIDS and STRUCTURES

www.elsevier.com/locate/ijsolstr

The helicoidal modeling in computational finite elasticity. Part II: Multiplicative interpolation

T. Merlini *, M. Morandini [1]

Dipartimento di Ingegneria Aerospaziale, Politecnico di Milano, Via La Masa 34, I-20158 Milano, Italy

Received 23 May 2003; received in revised form 9 February 2004
Available online 6 May 2004

Abstract

The approximate, substitute model of the position and orientation fields over a finite, multi-coordinate domain is built in a consistent way with the helicoidal modeling of the continuum, as proposed in Part I for a discrete application of variational principles in computational elasticity. The set of the position and orientation, referred to as oriento-position, is made dependent multiplicatively on the nodal values through relative rototranslations, and an implicit interpolation formula is written by weighting the relative helices. The proposed interpolation scheme is frame-invariant and path-independent, and the resulting weighted average oriento-position is obtained numerically. A consistent linearization of the model field is carried out by developing explicit formulae for the derivatives, up to third-order, of orthogonal tensors. The parent interpolation of the orientation field, which can be useful by itself in the context of classical modeling, is also discussed.

Keywords: Interpolation; Finite rotations; Exponential map; Rototranslations; Dual algebra

1. Introduction

In the finite-element approximation of a variational principle, the process of making a field of variables dependent on a discrete number of variables, is referred to as interpolation among the nodal values. This process yields a model of the field to substitute for the actual field over the element domain. Of course, the model is expected to be consistent, i.e. respectful of the algebraic rules peculiar to the space to which the variables pertain. When the variables belong to a special orthogonal manifold as the particle orientations or the particle oriento-positions do (see Part I), then the non-commutative and multiplicative character of the composition of rotations and rototranslations must be preserved in the model and borne in mind during its

* Corresponding author. Tel.: +39-02-2399-8352; fax: +39-02-2399-8334.
E-mail addresses: teodoro.merlini@polimi.it (T. Merlini), marco.morandini@polimi.it (M. Morandini).
[1] Tel.: +39-02-2399-8362; fax: +39-02-2399-8334.

0020-7683/$ - see front matter © 2004 Elsevier Ltd. All rights reserved.
doi:10.1016/j.ijsolstr.2004.02.026

differentiation. In such a sense the interpolation of the orientation and oriento-position fields ought to be multiplicative, i.e. based on the relative rotation, or relative rototranslation, of any particle from the nodal orientations or oriento-positions, respectively.

In this paper we develop a multiplicative interpolation scheme capable of determining either the orientation or the oriento-position of a frame over a multi-coordinate domain from any number of given frames. The present formulation constitutes the consistent extension to multi-coordinate domains of a multiplicative interpolation available for the case of frames defined over a one-coordinate domain. A formula for interpolating sections on space-curved beams was first proposed by Borri and Bottasso (1994a,b). A similar multiplicative interpolation for beam elements has been independently developed by Crisfield and Jelenić (1999) and Jelenić and Crisfield (1999). More recently, Borri et al. (2000) rephrased their interpolation with a description of the configuration that coincides, although with a different formalism, with the one adopted in this work. Such interpolations have been successfully exploited both in beam elasticity problems and in rigid body dynamics (in the latter case, the coordinate is the time instead of the section abscissa). The multiplicative interpolation we propose for solid domains is based on the relative rotations, or relative rototranslations, from the nodal frames and so it is, by design, frame-indifferent and invariant under superposed rigid-body motion. Since no motion of the nodal frames is involved, the interpolation also guarantees path-independent solutions. This is in contrast with most of the commonly adopted interpolations, that miss either the property of frame invariance or that of path-independence (Crisfield and Jelenić, 1999; Jelenić and Crisfield, 1999). The proposed interpolation is governed by an implicit nonlinear statement and relies on a numerical solution, which however proves rather efficient.

While obtaining an interpolated orientation, or oriento-position, is by itself a quite simple problem to solve, the linearization of the model field turns out to be a much harder problem. For the purposes of a finite-element approximation, a threefold linearization is needed, involving spatial, virtual and incremental variations. Such variations are unavoidably coupled in the case of a field of orthogonal tensors, and entail mixed differentiations up to third-order, for a total of seven differentiations. The aim of the linearization process of the multiplicative interpolation is to tie the seven independent differential vectors or tensors characterizing such differentiations to the relevant nodal variation variables. The main difficulty in this process is to establish the relations between differential rotation vectors and variations of rotation vectors, or between differential helices and variations of helices for the case of rototranslations. This is a quite difficult task, involving the derivatives of the exponential map and yielding the associated differential maps. The interest in the computation of the derivatives of the exponential map is alive nowadays, as evidenced by a number of recent works (Rosati, 1999; de Souza Neto, 2001; Ortiz et al., 2001; Ritto-Corrêa and Camotim, 2002; see also Itskov, 2000, 2002; Itskov and Aksel, 2002). In order to evaluate the needed derivatives, we introduce an original, recursive representation of orthonormal tensors by means of an infinite family of so-called nesting tensors, which make it easier to differentiate up to any order the rotation and the rototranslation tensors in the context of vectorial parameterizations.

The formulation developed in this paper for a consistent kinematical field is based on the helicoidal modeling of the continuum as described in Part I. It can cope with arbitrarily large displacements and rotations, and will be used in Part III to build finite elements capable of large curvatures and suitable for geometrically nonlinear analyses. In Section 2, the multiplicative interpolation of the orientation field is formulated and the relevant properties are discussed. Section 3 gives the extension to the helicoidal interpolation of the oriento-position field. The linearization of the model field is accomplished in Section 4. In Section 5 the computational algorithm is discussed, and the linearization formulae are numerically verified. Finally, an example of interpolation is given in Section 6 and conclusions are drawn in Section 7. The formulation of the differential maps is outlined in Appendix A (case of rotations) and Appendix B (case of rototranslations).

2. Weighted average orientation

Let us concentrate on some well-known underlying features that characterize positions and orientations. Positions of points in space are measured by distances, while orientations of frames are measured by relative rotations, and such geometrical measures are deeply different in character. Distances are elements of the linear Euclidean vector space, and so they commute and sum up additively, while rotations belong to the group of special orthogonal transformations, hence they do not commute and compose multiplicatively. Now, consider the problem of interpolating a position or an orientation among given data. As far as the position is concerned, the simplest interpolation is achieved by looking for a *weighted average position* based on weighted distances, i.e. by solving the equation

$$\sum_{J=1}^{N} W_J(\boldsymbol{x} - \boldsymbol{x}_J) = \boldsymbol{0}. \tag{1}$$

Eq. (1) gives the position vector $\boldsymbol{x}$ of the point with null weighted average of distances from N given points with position vectors $\boldsymbol{x}_J$ and weights $W_J (J = 1, 2, \ldots, N)$. By exploiting the same concept, an interpolated orientation can be sought as a *weighted average orientation* based on appropriate weighted 'distances', such to measure the relative orientations in a way consistent with the special orthogonal manifold to which rotations belong. By recalling the exponential map of the rotation and the inverse logarithmic map (namely $\boldsymbol{\Phi} = \exp(\boldsymbol{\varphi}\times)$ and $\boldsymbol{\varphi}\times = \log \boldsymbol{\Phi}$, see Part I), the most natural choice for such 'distance' appears to be the logarithm of the relative rotation from a given frame. Therefore, the following equation is written,

$$\sum_{J=1}^{N} W_J \log(\boldsymbol{\alpha}\boldsymbol{\alpha}_J^{\mathrm{T}}) = \boldsymbol{0}, \tag{2}$$

forcing to zero the weighted average of the logarithms of the rotation tensors from N given frames, with orientation tensors $\boldsymbol{\alpha}_J$ and weights W_J, to a frame with orientation tensor $\boldsymbol{\alpha}$. Although not strictly necessary, it is understood throughout the paper that the frames are made of orthonormal triads, and that brings the orientation tensors to be actually rotation tensors.

Eqs. (1) and (2) state the appropriate interpolation schemes for either kinds of fields. We can interpret the position $\boldsymbol{x}$ as the *sum* of a known position $\boldsymbol{x}_J$ plus the distance $\boldsymbol{x} - \boldsymbol{x}_J$, and we can do so N times. The linear Eq. (1) weighs such distances and gives the interpolated position in closed form, $\boldsymbol{x} = \sum W_J \boldsymbol{x}_J$ for normalized weights. This is an *additive* interpolation scheme. Analogously, the orientation $\boldsymbol{\alpha}$ is interpreted N times as a known orientation $\boldsymbol{\alpha}_J$ *multiplied* by a relative rotation $\tilde{\boldsymbol{\Phi}}_J = \boldsymbol{\alpha}\boldsymbol{\alpha}_J^{\mathrm{T}}$, see Fig. 1 (where, for clarity,

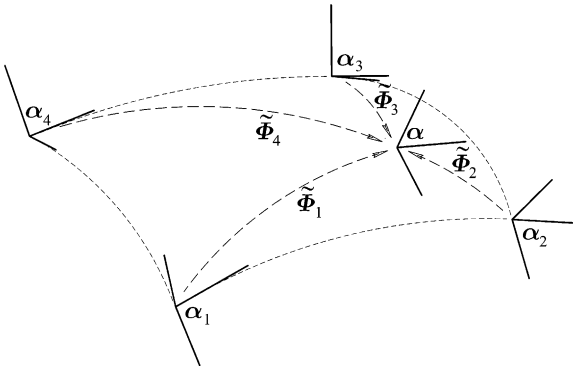

Fig. 1. Example of multiplicative interpolation of the orientation.

the frames are kept separate in space). Eq. (2) weighs the logarithms $\tilde{\boldsymbol{\varphi}}_J\times = \log\tilde{\boldsymbol{\Phi}}_J$, hence the relative rotation vectors $\tilde{\boldsymbol{\varphi}}_J = \operatorname{ax}\log\tilde{\boldsymbol{\Phi}}_J$; however, Eq. (2) is an implicit nonlinear equation and cannot give in general the interpolated orientation $\boldsymbol{\alpha}$ in closed form, but needs a numerical solution (see Section 5.1). This is a *multiplicative* interpolation scheme.

The interpolation scheme of Eq. (2) is *objective*. In order to ascertain the frame indifference, consider the reference frame back-rotated by a rotation $\boldsymbol{\beta}^{\mathrm{T}}$, so that the orientations of the given frames are represented by orientation tensors $\hat{\boldsymbol{\alpha}}_J = \boldsymbol{\alpha}_J\boldsymbol{\beta}$. Then, application of Eq. (2) yields a weighted average orientation $\hat{\boldsymbol{\alpha}} = \boldsymbol{\alpha}\boldsymbol{\beta}$, representing the same interpolated frame with respect to the new reference frame. This ensures the frame indifference of the interpolation scheme. Manifestly, the interpolation scheme is also invariant for superposed rigid motion; e.g. for new, rigidly rotated orientation tensors $\hat{\boldsymbol{\alpha}}_J = \boldsymbol{\beta}\boldsymbol{\alpha}_J$, the weighted average orientation becomes $\hat{\boldsymbol{\alpha}} = \boldsymbol{\beta}\boldsymbol{\alpha}$. This is easily checked using the identities $\boldsymbol{\Psi}\exp(\boldsymbol{\varphi}\times)\boldsymbol{\Psi}^{\mathrm{T}} = \exp(\boldsymbol{\Psi}\boldsymbol{\varphi}\times\boldsymbol{\Psi}^{\mathrm{T}}) = \exp((\boldsymbol{\Psi}\boldsymbol{\varphi})\times)$ and $\log(\boldsymbol{\Psi}\boldsymbol{\Phi}\boldsymbol{\Psi}^{\mathrm{T}}) = \boldsymbol{\Psi}(\log\boldsymbol{\Phi})\boldsymbol{\Psi}^{\mathrm{T}}$, valid for any two orthonormal tensors $\boldsymbol{\Phi}$ and $\boldsymbol{\Psi}$.

In spite of the analogy of the definitions of weighted average position and weighted average orientation, the multiplicative character of the composition of rotations entails an important consequence about the significance of averaging rotation tensors. After assigning arbitrary displacements to the given points, or arbitrary rotations to the given frames, it is seen that the displacement of the interpolated position coincides with the weighted average of the displacements of the given points, while the rotation of the interpolated orientation does not correspond in general to the weighted average of the rotations of the given frames. Let us see this in detail. By moving $\boldsymbol{x}_J$ to new positions $\boldsymbol{x}'_J = \boldsymbol{x}_J + \boldsymbol{u}_J$ and interpolating by Eq. (1) $\boldsymbol{x}' = \sum W_J\boldsymbol{x}'_J$, one computes a displacement $\boldsymbol{u} = \boldsymbol{x}' - \boldsymbol{x}$ coincident with the weighted average displacement, $\boldsymbol{u} = \sum W_J\boldsymbol{u}_J$. On the contrary, by rotating $\boldsymbol{\alpha}_J$ to new orientations $\boldsymbol{\alpha}'_J = \boldsymbol{\Phi}_J\boldsymbol{\alpha}_J$ and using Eq. (2) to interpolate $\boldsymbol{\alpha}'$ from $\sum W_J\log(\boldsymbol{\alpha}'\boldsymbol{\alpha}_J^{\mathrm{T}}\boldsymbol{\Phi}_J^{\mathrm{T}}) = \boldsymbol{0}$, one obtains a rotation $\boldsymbol{\Phi} = \boldsymbol{\alpha}'\boldsymbol{\alpha}^{\mathrm{T}}$ that in general does *not* correspond to any kind of 'weighted average rotation' of the rotations $\boldsymbol{\Phi}_J$. It can be argued that in the Euclidean linear space, averaging the displacements of *different* points, is consistent with averaging the point positions; on the special orthogonal manifold, instead, averaging the rotations of *different* frames, is in general *inconsistent* with averaging the frame orientations. However, in few particular cases the rotation of the weighted average orientation coincides with the weighted average of the rotations from the given orientations, as obtained by solving the equation $\sum W_J\log(\boldsymbol{\Phi}\boldsymbol{\Phi}_J^{\mathrm{T}}) = \boldsymbol{0}$. It is easy to see that this is true (i) when the orientations of the given frames coincide to each other (case of rotations from a common orientation, $\boldsymbol{\alpha} \equiv \boldsymbol{\alpha}_1 \equiv \boldsymbol{\alpha}_2 \equiv \cdots \equiv \boldsymbol{\alpha}_N$), (ii) when all the given frames undergo a unique rotation (rigid rotation, $\boldsymbol{\Phi} \equiv \boldsymbol{\Phi}_1 \equiv \boldsymbol{\Phi}_2 \equiv \cdots \equiv \boldsymbol{\Phi}_N$) and (iii) when the rotations are coaxial (a direction $\boldsymbol{n}$ exists such that $\boldsymbol{\Phi}\boldsymbol{n} \equiv \boldsymbol{\Phi}_1\boldsymbol{n} \equiv \boldsymbol{\Phi}_2\boldsymbol{n} \equiv \cdots \equiv \boldsymbol{\Phi}_N\boldsymbol{n} \equiv \boldsymbol{n}$), hence they commute and sum up (for instance, the planar case).

These considerations are quite important and permeate the whole interpolation philosophy we follow in a nonlinear finite element context. The local orientation is interpolated among the nodal orientations in the same way in either the initial configuration or a deformed configuration, and the angular curvature (which characterizes the gradient of the orientation, $\boldsymbol{k}_{\mathrm{a}} = \boldsymbol{\alpha}\operatorname{ax}(\boldsymbol{\alpha}^{\mathrm{T}}\boldsymbol{\alpha}_{/\otimes})$, see Part I) is computed from the nodal orientations in the same way in either configurations. No interpolation is attempted among the nodal rotations nor an angular strain is directly computed from them. The local rotation is recovered by comparing the local orientations in the deformed and initial configurations, and the angular strain is computed as the appropriate change of angular curvature (Part I, $\boldsymbol{\omega}_{\mathrm{a}} = \boldsymbol{k}'_{\mathrm{a}} - \boldsymbol{\Phi}\boldsymbol{k}_{\mathrm{a}}$). Since the local orientation and curvature are computed independently from the past history of the nodal orientations, our objective interpolation scheme is also intrinsically *path-independent*. As the frame invariance is achieved by averaging relative rotations, the path independence is closely related with the guess of interpolating orientations instead of their evolution, i.e. rotations.

This philosophy departs from the standard interpolation schemes adopted in finite elasticity. It is customary, when using a vectorial parameterization of the rotation, to rely on additive interpolations of either the total rotation vector or an incremental rotation vector. Consider, with the present notation and assuming orthonormal orientation tensors, the following interpolation formula,

$$\sum_{J=1}^{N} W_J(\log \boldsymbol{\alpha} - \log \boldsymbol{\alpha}_J) = \mathbf{0}. \tag{3}$$

By introducing the inverse exponential map $\boldsymbol{y}\times = \log \boldsymbol{\alpha}$, Eq. (3) yields the rotation vector defining the orientation $\boldsymbol{\alpha}$ in closed form, $\boldsymbol{y} = \sum W_J \boldsymbol{y}_J$. This interpolation does not depend on the evolution of the given frames, so it is path-independent. However, it is not frame-indifferent in three-dimensional space. In fact, by applying Eq. (3) to the orientations $\hat{\boldsymbol{\alpha}}_J = \boldsymbol{\alpha}_J \boldsymbol{\beta}$, measured from a reference frame back-rotated by $\boldsymbol{\beta}^{\mathrm{T}}$, the consistent orientation $\hat{\boldsymbol{\alpha}} = \boldsymbol{\alpha}\boldsymbol{\beta}$ cannot in general be achieved, simply because the rotation vector of the composition of two subsequent rotations is not the sum of the respective rotation vectors. This kind of interpolation is often cast in terms of rotations from the initial configuration (total rotations), see e.g. Cardona and Geradin (1988), Ibrahimbegović et al. (1995), Ritto-Corrêa and Camotim (2002); in these formulations, it coincides with Eq. (3) if the initial orientations are identical. Alternatively, the incremental rotation (from a converged solution) or the iterative rotation (during the solution process) is interpolated with the additive formula $\boldsymbol{y}_\partial = \sum W_J \boldsymbol{y}_{\partial J}$, and used to update the total rotation (refer to Jelenić and Crisfield, 1999, and to works quoted therein). The invariance of some incremental/iterative interpolations under superposed rigid-body motion has been recently proved by Ibrahimbegović and Taylor (2002) with a detailed analysis. However, it is common notion that additive interpolations of incremental/iterative rotations lead to path-dependent solutions.

The non-invariance and/or path-dependence of the additive interpolation schemes is discussed deeply by Crisfield and Jelenić (1999) and Jelenić and Crisfield (1999). They conclude that none of the commonly used interpolation formulae can ensure frame invariance and path independence at the same time. In their work—which however deals only with beam elements—they propose to interpolate the relative rotation vectors from an appropriate reference frame, properly tied to the nodal orientations. By this way, they are able to release the interpolation from the evolution of the nodal orientations, so attaining at the same time frame-invariance and path-independence. This interpolation scheme is in agreement with the one-dimensional helicoidal interpolation already published by Borri and Bottasso (1994a,b) in the modeling of space-curved beams. The scheme we propose in the present work can be seen as the extension to multi-coordinate domains of such kind of multiplicative interpolation, together with a systematic linearization that was lacking in that works.

3. Weighted average oriento-position

Oriento-positions in space are measured by rototranslations, and rototranslations are orthonormal dual tensors belonging to a special orthogonal group (see Part I). We denote with $\boldsymbol{H} = \exp(\boldsymbol{\eta}\times)$ and $\boldsymbol{\eta}\times = \log \boldsymbol{H}$ the exponential and logarithmic maps of a rototranslation $\boldsymbol{H}$, of helix $\boldsymbol{\eta}$. A dual tensor $\boldsymbol{A} = \boldsymbol{X}\boldsymbol{\alpha} = (\boldsymbol{I} + \varepsilon \boldsymbol{x}\times)\boldsymbol{\alpha}$ represents an oriento-position, which is assumed orthonormal so that $\boldsymbol{A}\boldsymbol{A}^{\mathrm{T}} = \boldsymbol{I}$. Owing to the close analogy with orientation and rotation tensors, and thanks to the powerful formalism of the algebra of dual numbers (Angeles, 1998), the extension of the concept of weighted average orientation to the case of the oriento-position is straightforward. In this case, the 'distance' on which the *weighted average oriento-position* is based is the logarithm of the relative rototranslation from a given applied frame, i.e. the relative helix. The interpolation is therefore referred to as *helicoidal interpolation* and is governed by the equation

$$\sum_{J=1}^{N} W_J \log(\boldsymbol{A}\boldsymbol{A}_J^{\mathrm{T}}) = \mathbf{0}. \tag{4}$$

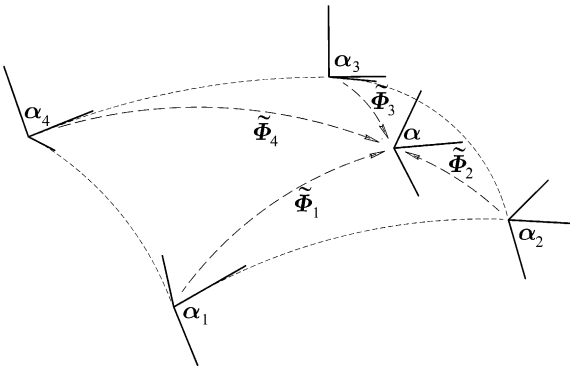

Fig. 2. Example of multiplicative interpolation of the oriento-position.

Eq. (4) forces to zero the weighted average of the logarithms of the rototranslation tensors from N given applied frames, with oriento-position tensors $\boldsymbol{A}_J$ and weights W_J, to an applied frame with oriento-position tensor $\boldsymbol{A}$.

As for the case of the orientation, we observe that the interpolation scheme is *multiplicative*: for N times, the oriento-position $\boldsymbol{A}$ is a known oriento-position $\boldsymbol{A}_J$ *multiplied* by a relative rototranslation $\tilde{\boldsymbol{H}}_J = \boldsymbol{A}\boldsymbol{A}_J^{\mathrm{T}}$, and Eq. (4) is weighing the logarithms $\tilde{\boldsymbol{\eta}}_J \times = \log \tilde{\boldsymbol{H}}_J$, hence the relative helices $\tilde{\boldsymbol{\eta}}_J = \mathrm{ax}\log \tilde{\boldsymbol{H}}_J$. The scheme is depicted in Fig. 2, where now the location in space of the frames is pertinent. In the example of Fig. 2, we can also compare the present interpolation, originating from the helicoidal modeling, with the classical independent interpolations of the position and orientation fields (dash sketch); in the latter case, the same orientation (note that the primal part of dual tensor $\boldsymbol{A}$ is just the orientation $\boldsymbol{\alpha}$) is located in a position independently interpolated among the given positions. In the helicoidal interpolation, of course, the implicit nonlinear Eq. (4) must be solved numerically for the oriento-position $\boldsymbol{A}$ (see Section 5.2).

By the same arguments as for Eq. (2), we infer that the interpolation scheme of Eq. (4) is *objective*. Moreover, it is seen that, after assigning arbitrary rototranslations to the given applied frames, the rototranslation of the interpolated oriento-position does not correspond in general to the weighted average of the rototranslations of the given applied frames. This confirms that averaging the rototranslations of *different* applied frames is in general *inconsistent* with averaging the frame oriento-positions. However, the rototranslation of the weighted average oriento-position coincides with the weighted average of the rototranslations in three particular cases: (i) obviously, when the rototranslations depart from a common oriento-position; (ii) when the rototranslation is unique for all the given applied frames, that is when the motion is rigid; (iii) when rototranslations are coaxial, and the interpolation becomes controlled by a scalar equation involving dual magnitudes of helices that commute and sum up. Again, by keeping to the interpolation of oriento-positions instead of rototranslations, an intrinsically *path-independent* scheme is achieved.

4. Linearization of the model field

In view of the formulation of finite elements, it is important to be able to differentiate the model of the kinematical field of orthonormal tensors set up by the interpolation scheme, with respect to either the spatial, virtual and incremental variations. In the differentiation process, we extend the formulation up to the relationship among the *local variation variables* and the *nodal variation variables*. In fact, we can, and

shall avoid choosing the actually free variables representing the nodal orthonormal tensors, so we do not reach linear expressions with respect to the free-variable variations. In a sense, this differentiation process is the parameterization-free core of the linearization; nevertheless, we shortly refer to it as the (threefold) linearization of the interpolation. Indeed, it should be pointed out here that the choice of a parameterization is still unavoidable for the differentiation of the relative rotation (or rototranslation) field inside the interpolation domain, and for this purpose we will resort to the natural parameterization based on the exponential map.

The linearization of the proposed interpolation of an orthonormal field is identical for the cases of orientations and oriento-positions. In the present context of the helicoidal modeling, we just refer to the case of the oriento-position field. The reader interested in linearizing the interpolation of the orientation field can follow the present derivation and substitute orientations for oriento-positions, rotations for rototranslations, and so on, and drop any reference to dual quantities. For the present case, the linearization can be outlined as follows. The spatial, virtual and incremental variations of the oriento-position field are coupled because of the inherent nonlinearity in the representation of rototranslations (see Part I), and entail mixed differentiations up to third-order for a total of seven differentiations. Seven independent differential dual vectors or tensors characterize such differentiations. Such local variation variables are related to the appropriate nodal variation variables by the linearization of the multiplicative model of the kinematical field, through appropriate *relative variation variables*, so that the couplings among the variation variables are consistently preserved.

In a finite element context, we are concerned with interpolation within a continuum. We describe the domain of interest by means of a number n of material coordinates, say $\xi^i (i = 1, 2, \ldots, n)$; typically, $n = 3$ for a three-dimensional solid, $n = 2$ on a surface (shells) and $n = 1$ along a line (beams). The weights W_J are N scalar functions of the domain coordinates, normalized so that $\sum W_J = 1$ everywhere; they are known functions, and so are their derivatives $W_{J,i}$ with respect to the domain coordinates. The notation $(\ )_{/\otimes} \equiv (\ )_{,i} \otimes \boldsymbol{g}^i$ means the gradient, so $W_{J/\otimes}$ are the gradients of functions W_J. The oriento-position field is defined as a dual tensor function of the abstract placement identified by a set of values of the coordinates within the domain, symbolically $\boldsymbol{A} = \boldsymbol{A}(\xi^1, \xi^2, \ldots, \xi^n)$. On the other hand, $\boldsymbol{A}_J$ are the nodal oriento-positions at N abstract placements identified by some coordinates ξ^i_J, and are assumed as known. In this paper, we implicitly refer to the case of three-dimensional solids ($n = 3$). However, accounting for a different number of coordinates is immediate.

4.1. Local and nodal variation variables

The quantities to be considered in the interpolation are the oriento-position $\boldsymbol{A}$ itself, its virtual, incremental and mixed virtual-incremental variations $\delta\boldsymbol{A}$, $\partial\boldsymbol{A}$, $\partial\delta\boldsymbol{A}$, the finite gradient $\boldsymbol{A}_{/\otimes}$ and the relevant virtual, incremental and mixed virtual-incremental variations $\delta\boldsymbol{A}_{/\otimes}$, $\partial\boldsymbol{A}_{/\otimes}$, $\partial\delta\boldsymbol{A}_{/\otimes}$. Since the spatial, virtual and incremental variations are independent of each other, the mixed changes involve differentiations up to the third-order. A study of the differentiation of rototranslation tensors (see Part I and Merlini, 2002) yields appropriate expressions for such variations, which we group in the following scheme, where we enclose the orthogonality condition for the sake of completeness:

$$\begin{aligned}
\boldsymbol{A}^{\mathrm{T}}\boldsymbol{A} &= \boldsymbol{I} \\
\boldsymbol{A}^{\mathrm{T}}\delta\boldsymbol{A} &= (\boldsymbol{A}^{\mathrm{T}}\boldsymbol{a}_{\delta})\times \\
\boldsymbol{A}^{\mathrm{T}}\partial\boldsymbol{A} &= (\boldsymbol{A}^{\mathrm{T}}\boldsymbol{a}_{\partial})\times \\
\boldsymbol{A}^{\mathrm{T}}\partial\delta\boldsymbol{A} &= (\boldsymbol{A}^{\mathrm{T}}\boldsymbol{a}_{\partial\delta})\times + \frac{1}{2}((\boldsymbol{A}^{\mathrm{T}}\boldsymbol{a}_{\partial})\times(\boldsymbol{A}^{\mathrm{T}}\boldsymbol{a}_{\delta})\times + (\boldsymbol{A}^{\mathrm{T}}\boldsymbol{a}_{\delta})\times(\boldsymbol{A}^{\mathrm{T}}\boldsymbol{a}_{\partial})\times)
\end{aligned} \tag{5}$$

and

$$
\begin{aligned}
\boldsymbol{A}^{\mathrm{T}}\boldsymbol{A}_{/\otimes} &= (\boldsymbol{A}^{\mathrm{T}}\boldsymbol{k})^{\times}\\
\boldsymbol{A}^{\mathrm{T}}\delta\boldsymbol{A}_{/\otimes} &= (\boldsymbol{A}^{\mathrm{T}}\boldsymbol{k}_{\delta})^{\times} - \frac{1}{2}((\boldsymbol{A}^{\mathrm{T}}\boldsymbol{a}_{\delta})\times\boldsymbol{A}^{\mathrm{T}}\boldsymbol{k})^{\times} + (\boldsymbol{A}^{\mathrm{T}}\boldsymbol{a}_{\delta})\times(\boldsymbol{A}^{\mathrm{T}}\boldsymbol{k})^{\times}\\
\boldsymbol{A}^{\mathrm{T}}\partial\boldsymbol{A}_{/\otimes} &= (\boldsymbol{A}^{\mathrm{T}}\boldsymbol{k}_{\partial})^{\times} - \frac{1}{2}((\boldsymbol{A}^{\mathrm{T}}\boldsymbol{a}_{\partial})\times\boldsymbol{A}^{\mathrm{T}}\boldsymbol{k})^{\times} + (\boldsymbol{A}^{\mathrm{T}}\boldsymbol{a}_{\partial})\times(\boldsymbol{A}^{\mathrm{T}}\boldsymbol{k})^{\times}\\
\boldsymbol{A}^{\mathrm{T}}\partial\delta\boldsymbol{A}_{/\otimes} &= (\boldsymbol{A}^{\mathrm{T}}\boldsymbol{k}_{\partial\delta})^{\times} - \frac{1}{2}((\boldsymbol{A}^{\mathrm{T}}\boldsymbol{a}_{\partial\delta})\times\boldsymbol{A}^{\mathrm{T}}\boldsymbol{k})^{\times} + (\boldsymbol{A}^{\mathrm{T}}\boldsymbol{a}_{\partial\delta})\times(\boldsymbol{A}^{\mathrm{T}}\boldsymbol{k})^{\times}\\
&\quad - \frac{1}{2}((\boldsymbol{A}^{\mathrm{T}}\boldsymbol{a}_{\partial})\times\boldsymbol{A}^{\mathrm{T}}\boldsymbol{k}_{\delta} + (\boldsymbol{A}^{\mathrm{T}}\boldsymbol{a}_{\delta})\times\boldsymbol{A}^{\mathrm{T}}\boldsymbol{k}_{\partial})^{\times} + (\boldsymbol{A}^{\mathrm{T}}\boldsymbol{a}_{\partial})\times(\boldsymbol{A}^{\mathrm{T}}\boldsymbol{k}_{\delta})^{\times} + (\boldsymbol{A}^{\mathrm{T}}\boldsymbol{a}_{\delta})\times(\boldsymbol{A}^{\mathrm{T}}\boldsymbol{k}_{\partial})^{\times}.
\end{aligned}
\tag{6}
$$

Seven differential dual tensors characterize the seven variations: the virtual, incremental and mixed virtual-incremental oriento-position vectors $\boldsymbol{a}_{\delta}$, $\boldsymbol{a}_{\partial}$, $\boldsymbol{a}_{\partial\delta}$, the finite curvature $\boldsymbol{k}$, and the virtual, incremental and mixed virtual-incremental curvatures $\boldsymbol{k}_{\delta}$, $\boldsymbol{k}_{\partial}$, $\boldsymbol{k}_{\partial\delta}$. Such characteristic variation variables are defined by Eqs. (5) and (6), and are representative of the axial vectors of second-order dual tensors like $\boldsymbol{A}^{\mathrm{T}}\delta\boldsymbol{A},\ldots$, and of the axial tensors of third-order dual tensors like $\boldsymbol{A}^{\mathrm{T}}\boldsymbol{A}_{/\otimes},\ldots$ They will be referred to as the *local variation variables* and constitute the outcome of the linearization process of the interpolation.

The interpolation is performed among the nodal oriento-positions $\boldsymbol{A}_J$. Furthermore, the relevant virtual, incremental and mixed virtual-incremental variations are considered. According to similar expressions

$$
\begin{aligned}
\boldsymbol{A}_J^{\mathrm{T}}\delta\boldsymbol{A}_J &= (\boldsymbol{A}_J^{\mathrm{T}}\boldsymbol{a}_{\delta J})\times\\
\boldsymbol{A}_J^{\mathrm{T}}\partial\boldsymbol{A}_J &= (\boldsymbol{A}_J^{\mathrm{T}}\boldsymbol{a}_{\partial J})\times\\
\boldsymbol{A}_J^{\mathrm{T}}\partial\delta\boldsymbol{A}_J &= (\boldsymbol{A}_J^{\mathrm{T}}\boldsymbol{a}_{\partial\delta J})\times + \frac{1}{2}((\boldsymbol{A}_J^{\mathrm{T}}\boldsymbol{a}_{\partial J})\times(\boldsymbol{A}_J^{\mathrm{T}}\boldsymbol{a}_{\delta J})\times + (\boldsymbol{A}_J^{\mathrm{T}}\boldsymbol{a}_{\delta J})\times(\boldsymbol{A}_J^{\mathrm{T}}\boldsymbol{a}_{\partial J})\times),
\end{aligned}
\tag{7}
$$

the virtual, incremental and mixed virtual-incremental nodal oriento-position vectors $\boldsymbol{a}_{\delta J}$, $\boldsymbol{a}_{\partial J}$, $\boldsymbol{a}_{\partial\delta J}$ characterize such variations. They are referred to as the *nodal variation variables* and constitute the input arguments of the interpolation linearization, to be regarded as independent variables.

It is worth discussing the presence of the mixed virtual-incremental variation variables $\boldsymbol{a}_{\partial\delta}$ and $\boldsymbol{k}_{\partial\delta}$ at a generic place, and $\boldsymbol{a}_{\partial\delta J}$ at the nodes. At the nodes, where the actually free variables of a problem are defined, the mixed variation variables $\boldsymbol{a}_{\partial\delta J}$ can, and will be solved for the simple variation variables $\boldsymbol{a}_{\delta J}$ and $\boldsymbol{a}_{\partial J}$, using the differential maps giving the variation variables from the variations of the actually free variables. At a generic internal place, where the variables are not actually free variables, but are nonlinearly dependent on the nodal free variables, the mixed variation variables $\boldsymbol{a}_{\partial\delta}$ and $\boldsymbol{k}_{\partial\delta}$ cannot be solved in a similar way for the relevant simple variation variables $\boldsymbol{a}_{\delta}$, $\boldsymbol{a}_{\partial}$, or $\boldsymbol{k}_{\delta}$, $\boldsymbol{k}_{\partial}$. Instead, they must be interpolated independently and undergo independent dependencies on $\boldsymbol{a}_{\partial\delta J}$.

4.2. Relative variation variables

Let us focus now on the relative rototranslations $\tilde{\boldsymbol{H}}_J = \boldsymbol{A}\boldsymbol{A}_J^{\mathrm{T}}$ from the known nodal oriento-positions to the interpolated local oriento-position, and on the relative helices defined as the dual axial vectors of the relevant skew-symmetric logarithmic maps, $\tilde{\boldsymbol{\eta}}_J = \mathrm{ax}\log\tilde{\boldsymbol{H}}_J$. The spatial, virtual and incremental variations of the relative rototranslations obey by themselves expressions analogous to Eqs. (5) and (6), that actually define seven characteristic differential dual tensors, referred to as the *relative variation variables*. They are the virtual, incremental and mixed virtual-incremental relative helices $\tilde{\boldsymbol{\eta}}_{\delta J}$, $\tilde{\boldsymbol{\eta}}_{\partial J}$, $\tilde{\boldsymbol{\eta}}_{\partial\delta J}$, the finite relative strain $\tilde{\boldsymbol{\omega}}_J$, and the virtual, incremental and mixed virtual-incremental relative strains $\tilde{\boldsymbol{\omega}}_{\delta J}$, $\tilde{\boldsymbol{\omega}}_{\partial J}$, $\tilde{\boldsymbol{\omega}}_{\partial\delta J}$. Here, we leave out the relevant defining formulae; they can be obtained from Eqs. (5) and (6), simply replacing $\boldsymbol{A}$ with $\tilde{\boldsymbol{H}}_J$, $\boldsymbol{a}$ with $\tilde{\boldsymbol{\eta}}_J$, and $\boldsymbol{k}$ with $\tilde{\boldsymbol{\omega}}_J$ everywhere.

The interpolated oriento-position can be understood as the unique result of N different compositions of rototranslations, namely the oriento-position of each node J followed by the relevant relative rototranslation, $\boldsymbol{A} = \tilde{\boldsymbol{H}}_J \boldsymbol{A}_J$. By taking the variations of the oriento-position field, the variations of either the relative rototranslations and the nodal oriento-positions are involved. By working on the equations defining the respective variation variables, it is possible to obtain, after complicated manipulations (Merlini, 2002), a relationship between the local variation variables, the relative variation variables and the nodal variation variables,

$$\begin{aligned}
\boldsymbol{a}_\delta &= \tilde{\boldsymbol{\eta}}_{\delta J} + \tilde{\boldsymbol{H}}_J \boldsymbol{a}_{\delta J} \\
\boldsymbol{a}_\partial &= \tilde{\boldsymbol{\eta}}_{\partial J} + \tilde{\boldsymbol{H}}_J \boldsymbol{a}_{\partial J} \\
\boldsymbol{a}_{\partial\delta} &= \tilde{\boldsymbol{\eta}}_{\partial\delta J} + \tilde{\boldsymbol{H}}_J \boldsymbol{a}_{\partial\delta J} - \frac{1}{2}((\tilde{\boldsymbol{H}}_J \boldsymbol{a}_{\partial J})\times\tilde{\boldsymbol{\eta}}_{\delta J} + (\tilde{\boldsymbol{H}}_J \boldsymbol{a}_{\delta J})\times\tilde{\boldsymbol{\eta}}_{\partial J})
\end{aligned} \tag{8}$$

and

$$\begin{aligned}
\boldsymbol{k} &= \tilde{\boldsymbol{\omega}}_J \\
\boldsymbol{k}_\delta &= \tilde{\boldsymbol{\omega}}_{\delta J} - \frac{1}{2}(\tilde{\boldsymbol{H}}_J \boldsymbol{a}_{\delta J})\times\tilde{\boldsymbol{\omega}}_J \\
\boldsymbol{k}_\partial &= \tilde{\boldsymbol{\omega}}_{\partial J} - \frac{1}{2}(\tilde{\boldsymbol{H}}_J \boldsymbol{a}_{\partial J})\times\tilde{\boldsymbol{\omega}}_J \\
\boldsymbol{k}_{\partial\delta} &= \tilde{\boldsymbol{\omega}}_{\partial\delta J} - \frac{1}{2}(\tilde{\boldsymbol{H}}_J \boldsymbol{a}_{\partial\delta J})\times\tilde{\boldsymbol{\omega}}_J - \frac{1}{2}((\tilde{\boldsymbol{H}}_J \boldsymbol{a}_{\partial J})\times\tilde{\boldsymbol{\omega}}_{\delta J} + (\tilde{\boldsymbol{H}}_J \boldsymbol{a}_{\delta J})\times\tilde{\boldsymbol{\omega}}_{\partial J}) \\
&\quad + \frac{1}{4}((\tilde{\boldsymbol{H}}_J \boldsymbol{a}_{\partial J})\times(\tilde{\boldsymbol{\eta}}_{\delta J} + \tilde{\boldsymbol{H}}_J \boldsymbol{a}_{\delta J})\times + (\tilde{\boldsymbol{H}}_J \boldsymbol{a}_{\delta J})\times(\tilde{\boldsymbol{\eta}}_{\partial J} + \tilde{\boldsymbol{H}}_J \boldsymbol{a}_{\partial J})\times)\tilde{\boldsymbol{\omega}}_J \\
&\quad - (\tilde{\boldsymbol{H}}_J \boldsymbol{a}_{\partial J} \otimes \tilde{\boldsymbol{\eta}}_{\delta J} + \tilde{\boldsymbol{H}}_J \boldsymbol{a}_{\delta J} \otimes \tilde{\boldsymbol{\eta}}_{\partial J} + \tilde{\boldsymbol{H}}_J \boldsymbol{a}_{\partial J} \otimes \tilde{\boldsymbol{H}}_J \boldsymbol{a}_{\delta J})^{\mathrm{S}} \cdot \tilde{\boldsymbol{\omega}}_J.
\end{aligned} \tag{9}$$

By means of Eqs. (8) and (9), the outcome of the linearization, i.e. the local variation variables, are made dependent on the relative variation variables. In the linearization process, we shall exploit the inverse relationship, obtained by solving Eqs. (8) and (9) for the relative variation variables.

4.3. Linearization equations

The linearization of the interpolation is accomplished by rewriting the statement of weighted average oriento-position, Eq. (4), in terms of the axial vectors of the logarithms of the relative rototranslations, i.e. the relative helices, and by differentiating it in either the spatial, virtual and incremental sense. We obtain the following equations, where the original statement is included for completeness:

$$\begin{aligned}
&\sum_{J=1}^{N} W_J \tilde{\boldsymbol{\eta}}_J = \boldsymbol{0}, \\
&\sum_{J=1}^{N} W_J \delta\tilde{\boldsymbol{\eta}}_J = \boldsymbol{0}, \\
&\sum_{J=1}^{N} W_J \partial\tilde{\boldsymbol{\eta}}_J = \boldsymbol{0}, \\
&\sum_{J=1}^{N} W_J \partial\delta\tilde{\boldsymbol{\eta}}_J = \boldsymbol{0}
\end{aligned} \tag{10}$$

and

$$\begin{aligned}
&\sum_{J=1}^{N}(\tilde{\boldsymbol{\eta}}_J \otimes W_{J/\otimes} + W_J\tilde{\boldsymbol{\eta}}_{J/\otimes}) = \mathbf{0},\\
&\sum_{J=1}^{N}(\delta\tilde{\boldsymbol{\eta}}_J \otimes W_{J/\otimes} + W_J\delta\tilde{\boldsymbol{\eta}}_{J/\otimes}) = \mathbf{0},\\
&\sum_{J=1}^{N}(\partial\tilde{\boldsymbol{\eta}}_J \otimes W_{J/\otimes} + W_J\partial\tilde{\boldsymbol{\eta}}_{J/\otimes}) = \mathbf{0},\\
&\sum_{J=1}^{N}(\partial\delta\tilde{\boldsymbol{\eta}}_J \otimes W_{J/\otimes} + W_J\partial\delta\tilde{\boldsymbol{\eta}}_{J/\otimes}) = \mathbf{0}.
\end{aligned} \tag{11}$$

Apart from the first equation—that gives the interpolated oriento-position, hence the relative helices $\tilde{\boldsymbol{\eta}}_J$ themselves—Eqs. (10) and (11) collect seven algebraic equations having as unknowns all the plain and mixed variations up to the third-order of the relative helices. They are the virtual, incremental and mixed virtual-incremental variations $\delta\tilde{\boldsymbol{\eta}}_J$, $\partial\tilde{\boldsymbol{\eta}}_J$, $\partial\delta\tilde{\boldsymbol{\eta}}_J$, the gradients $\tilde{\boldsymbol{\eta}}_{J/\otimes}$, and the virtual, incremental and mixed virtual-incremental gradients $\delta\tilde{\boldsymbol{\eta}}_{J/\otimes}$, $\partial\tilde{\boldsymbol{\eta}}_{J/\otimes}$, $\partial\delta\tilde{\boldsymbol{\eta}}_{J/\otimes}$. In order to state the problem in terms of local variation variables, which are related to the relative variation variables by Eqs. (8) and (9), we still need to link the relative variation variables to the variations of the relative helices.

Given the exponential map of the rototranslation and its dual vector argument, the helix, the mapping of the variations of the helix itself onto the differential helices that characterize the differentiations of a rototranslation tensor is referred to as the associated *differential mapping*. For the present purposes, we are interested in mixed differential maps up to the third level, hence we get involved with mixed differentiations up to third-order of the rototranslation tensor, that is by no means an easy task. Resorting to an original recursive representation of orthonormal tensors by means of an infinite family of nesting tensors was decisive in yielding manageable expressions for the needed differential maps. The formulation is extensively discussed in Merlini (2003) and is outlined in two Appendices. The spirit of the theory is developed in Appendix A, which deals with the differential maps of the rotation and can be useful by itself to people interested in interpolating just the orientation tensors. The main results for the differential maps of the rototranslation are recovered in Appendix B, where meaningful explicit expressions are also discussed.

Application of Eqs. (B.14) and (B.15) to the present case yields the following direct relations between the relative variation variables and the variations of the relative helices,

$$\begin{aligned}
\tilde{\boldsymbol{\eta}}_{\delta J} &= \tilde{\boldsymbol{\Lambda}}_J\delta\tilde{\boldsymbol{\eta}}_J\\
\tilde{\boldsymbol{\eta}}_{\partial J} &= \tilde{\boldsymbol{\Lambda}}_J\partial\tilde{\boldsymbol{\eta}}_J\\
\tilde{\boldsymbol{\eta}}_{\partial\delta J} &= \tilde{\boldsymbol{\Lambda}}_J\partial\delta\tilde{\boldsymbol{\eta}}_J + \tilde{\boldsymbol{\Lambda}}^{\underline{12}\underline{\underline{3}}}_{\mathrm{III}J} : \delta\tilde{\boldsymbol{\eta}}_J \otimes \partial\tilde{\boldsymbol{\eta}}_J
\end{aligned} \tag{12}$$

and

$$\begin{aligned}
\tilde{\boldsymbol{\omega}}_J &= \tilde{\boldsymbol{\Lambda}}_J\tilde{\boldsymbol{\eta}}_{J/\otimes}\\
\tilde{\boldsymbol{\omega}}_{\delta J} &= \tilde{\boldsymbol{\Lambda}}_J\delta\tilde{\boldsymbol{\eta}}_{J/\otimes} + \tilde{\boldsymbol{\Lambda}}^{\underline{12}\underline{\underline{3}}}_{\mathrm{III}J} : \delta\tilde{\boldsymbol{\eta}}_J \otimes \tilde{\boldsymbol{\eta}}_{J/\otimes}\\
\tilde{\boldsymbol{\omega}}_{\partial J} &= \tilde{\boldsymbol{\Lambda}}_J\partial\tilde{\boldsymbol{\eta}}_{J/\otimes} + \tilde{\boldsymbol{\Lambda}}^{\underline{12}\underline{\underline{3}}}_{\mathrm{III}J} : \partial\tilde{\boldsymbol{\eta}}_J \otimes \tilde{\boldsymbol{\eta}}_{J/\otimes}\\
\tilde{\boldsymbol{\omega}}_{\partial\delta J} &= \tilde{\boldsymbol{\Lambda}}_J\partial\delta\tilde{\boldsymbol{\eta}}_{J/\otimes} + \tilde{\boldsymbol{\Lambda}}^{\underline{12}\underline{\underline{3}}}_{\mathrm{III}J} : (\partial\delta\tilde{\boldsymbol{\eta}}_J \otimes \tilde{\boldsymbol{\eta}}_{J/\otimes} + \partial\tilde{\boldsymbol{\eta}}_J \otimes \delta\tilde{\boldsymbol{\eta}}_{J/\otimes} + \delta\tilde{\boldsymbol{\eta}}_J \otimes \partial\tilde{\boldsymbol{\eta}}_{J/\otimes})\\
&\quad + \left(\tilde{\boldsymbol{\Lambda}}^{\underline{12}\underline{\underline{3}}\underline{\underline{\underline{4}}}}_{\mathrm{IV}J} - \left(\frac{1}{2}(\boldsymbol{I}^{\times}\tilde{\boldsymbol{\Lambda}}_J)^{\mathrm{T}132}\tilde{\boldsymbol{\Lambda}}^{\underline{12}\underline{\underline{3}}}_{\mathrm{III}J} + \tilde{\boldsymbol{\Lambda}}_J \otimes \tilde{\boldsymbol{\Lambda}}_J^{\mathrm{T}}\tilde{\boldsymbol{\Lambda}}_J\right)^{\mathrm{S}\underline{12}\underline{\underline{3}}\underline{\underline{\underline{4}}}}\right) \vdots \delta\tilde{\boldsymbol{\eta}}_J \otimes \partial\tilde{\boldsymbol{\eta}}_J \otimes \tilde{\boldsymbol{\eta}}_{J/\otimes},
\end{aligned} \tag{13}$$

and the inverse relations, that represent the solution of Eqs. (12) and (13) for the variations of the relative helices. Expressions for the mapping tensors, in either the direct form, $\tilde{\boldsymbol{\Lambda}}_J$, $\tilde{\boldsymbol{\Lambda}}_{\mathrm{III}J}^{\underline{12}\underline{3}}$, $\tilde{\boldsymbol{\Lambda}}_{\mathrm{IV}J}^{\underline{12}\underline{3}\underline{4}}$, and the inverse form, $\tilde{\boldsymbol{\Lambda}}_J^{-1}$, $\tilde{\boldsymbol{\Lambda}}_{\mathrm{III}J}^{-1\underline{1}\underline{2}}$, $\tilde{\boldsymbol{\Lambda}}_{\mathrm{IV}J}^{-1\underline{2}\underline{3}\underline{4}}$, are given in Appendix B, see Eqs. (B.16) and (B.17). Refer to Appendix A for an explanation of the notation used to denote particular symmetries of higher-order tensors.

4.4. Interpolation formulae

Within Eqs. (10) and (11), we now substitute the inverse of Eqs. (12) and (13) for the variations of the relative helices; then, we substitute the inverse of Eqs. (8) and (9) for the relative variation variables. Seven algebraic equations are obtained with the local variation variables as unknowns. They are solved in cascade (refer to Merlini and Morandini (2003) for any details) and yield the virtual, incremental and mixed virtual-incremental oriento-position dual vectors

$$\begin{aligned}
\boldsymbol{a}_{\delta} &= \sum_{J=1}^{N} \boldsymbol{V}_J \cdot \boldsymbol{a}_{\delta J},\\
\boldsymbol{a}_{\partial} &= \sum_{K=1}^{N} \boldsymbol{V}_K \cdot \boldsymbol{a}_{\partial K},\\
\boldsymbol{a}_{\partial\delta} &= \sum_{J=1}^{N} \boldsymbol{V}_J \cdot \boldsymbol{a}_{\partial\delta J} + \sum_{J=1}^{N}\sum_{K=1}^{N} \mathscr{V}_{JK} : \boldsymbol{a}_{\delta J} \otimes \boldsymbol{a}_{\partial K},
\end{aligned} \tag{14}$$

the finite curvature

$$\boldsymbol{k} = -\boldsymbol{\Lambda}_{\mathrm{II}}^{-\underline{\underline{1}}} \sum_{J=1}^{N} W_{J,i} \tilde{\boldsymbol{\eta}}_J \otimes \boldsymbol{g}^i \tag{15}$$

and the virtual, incremental and mixed virtual-incremental curvatures

$$\begin{aligned}
\boldsymbol{k}_{\delta} &= \sum_{J=1}^{N} \mathscr{W}_J : \boldsymbol{a}_{\delta J} \otimes \boldsymbol{I},\\
\boldsymbol{k}_{\partial} &= \sum_{K=1}^{N} \mathscr{W}_K : \boldsymbol{a}_{\partial K} \otimes \boldsymbol{I},\\
\boldsymbol{k}_{\partial\delta} &= \sum_{J=1}^{N} \mathscr{W}_J : \boldsymbol{a}_{\partial\delta J} \otimes \boldsymbol{I} + \sum_{J=1}^{N}\sum_{K=1}^{N} \mathbb{W}_{JK} \vdots \boldsymbol{a}_{\delta J} \otimes \boldsymbol{a}_{\partial K} \otimes \boldsymbol{I}.
\end{aligned} \tag{16}$$

The curvature $\boldsymbol{k}$ is obtained in closed form. The other local variation variables are obtainable by interpolation formulae linear with the nodal variation variables, i.e. the virtual, incremental and mixed virtual-incremental nodal oriento-position dual vectors $\boldsymbol{a}_{\delta J}$, $\boldsymbol{a}_{\partial J}$, $\boldsymbol{a}_{\partial\delta J}$. The coefficient dual tensors of the second, third and fourth-order in Eqs. (14) and (16) are given in closed form as

$$
\begin{aligned}
\boldsymbol{V}_J &= \boldsymbol{\Lambda}_{\mathrm{II}}^{-1}(W_J\tilde{\boldsymbol{\Lambda}}_J^{-1}\tilde{\boldsymbol{H}}_J),\\
\mathscr{V}_{JK} &= \boldsymbol{\Lambda}_{\mathrm{II}}^{-1}((\boldsymbol{\Lambda}_{\mathrm{III}}^{-1\underline{2}\underline{3}}\boldsymbol{V}_J)^{\mathrm{T}132}\boldsymbol{V}_K - (W_J\tilde{\boldsymbol{\Lambda}}_{J/}^{-\mathrm{T}132}\tilde{\boldsymbol{H}}_J)^{\mathrm{T}132}\boldsymbol{V}_K - ((W_K\tilde{\boldsymbol{\Lambda}}_{K/}^{-\mathrm{T}132}\tilde{\boldsymbol{H}}_K)^{\mathrm{T}132}\boldsymbol{V}_J)^{\mathrm{T}132}\\
&\qquad + \delta_{JK}(W_J\tilde{\boldsymbol{\Lambda}}_{\mathrm{III}J}^{-1\underline{2}\underline{3}}\tilde{\boldsymbol{H}}_J)^{\mathrm{T}132}\tilde{\boldsymbol{H}}_K)\\
&= \mathscr{V}_{KJ}^{\mathrm{T}132},\\
\mathscr{W}_J &= \boldsymbol{\Lambda}_{\mathrm{II}}^{-1}(-(\boldsymbol{\Lambda}_{\mathrm{II}/i}^{-} - \boldsymbol{\Lambda}_{\mathrm{III}}^{-1\underline{\underline{2}}\underline{\underline{3}}}\boldsymbol{k}_i)\boldsymbol{V}_J + (W_{J,i}\tilde{\boldsymbol{\Lambda}}_J^{-1} - W_J\tilde{\boldsymbol{\Lambda}}_{J/}^{-}\boldsymbol{k}_i)\tilde{\boldsymbol{H}}_J)\otimes\boldsymbol{g}^i,\\
\mathbb{W}_{JK} &= \boldsymbol{\Lambda}_{\mathrm{II}}^{-1}((\boldsymbol{\Lambda}_{\mathrm{III}}^{-1\underline{2}\underline{3}}\boldsymbol{V}_J - W_J\tilde{\boldsymbol{\Lambda}}_{J/}^{-\mathrm{T}132}\tilde{\boldsymbol{H}}_J)^{\mathrm{T}132}\mathscr{W}_{Ki} + ((\boldsymbol{\Lambda}_{\mathrm{III}}^{-1\underline{2}\underline{3}}\boldsymbol{V}_K - W_K\tilde{\boldsymbol{\Lambda}}_{K/}^{-\mathrm{T}132}\tilde{\boldsymbol{H}}_K)^{\mathrm{T}132}\mathscr{W}_{Ji})^{\mathrm{T}132}\\
&\qquad - (\boldsymbol{\Lambda}_{\mathrm{II}/i}^{-} - \boldsymbol{\Lambda}_{\mathrm{III}}^{-1\underline{\underline{2}}\underline{\underline{3}}}\boldsymbol{k}_i)\mathscr{V}_{JK} + ((\boldsymbol{\Lambda}_{\mathrm{III}/i}^{-1\underline{2}\underline{3}} + \boldsymbol{\Lambda}_{\mathrm{Q}}^{-1\underline{\underline{2}}\underline{\underline{3}}\underline{\underline{\underline{4}}}}\boldsymbol{k}_i)\boldsymbol{V}_J)^{\mathrm{T}132}\boldsymbol{V}_K\\
&\qquad - ((W_{J,i}\tilde{\boldsymbol{\Lambda}}_{J/}^{-\mathrm{T}132} + W_J(\tilde{\boldsymbol{\Lambda}}_{\mathrm{R}J}^{-1\underline{2}\underline{\underline{3}}\underline{\underline{\underline{4}}}} + \tilde{\boldsymbol{\Lambda}}_{\mathrm{Q}J}^{-1\underline{\underline{2}}\underline{\underline{3}}\underline{\underline{\underline{4}}}})\boldsymbol{k}_i)\tilde{\boldsymbol{H}}_J)^{\mathrm{T}132}\boldsymbol{V}_K\\
&\qquad - (((W_{K,i}\tilde{\boldsymbol{\Lambda}}_{K/}^{-\mathrm{T}132} + W_K(\tilde{\boldsymbol{\Lambda}}_{\mathrm{R}K}^{-1\underline{2}\underline{\underline{3}}\underline{\underline{\underline{4}}}} + \tilde{\boldsymbol{\Lambda}}_{\mathrm{Q}K}^{-1\underline{\underline{2}}\underline{\underline{3}}\underline{\underline{\underline{4}}}})\boldsymbol{k}_i)\tilde{\boldsymbol{H}}_K)^{\mathrm{T}132}\boldsymbol{V}_J)^{\mathrm{T}132}\\
&\qquad + \delta_{JK}((W_{J,i}\tilde{\boldsymbol{\Lambda}}_{\mathrm{III}J}^{-1\underline{2}\underline{3}} + W_J(\tilde{\boldsymbol{\Lambda}}_{\mathrm{L}J}^{-1\underline{2}\underline{\underline{3}}\underline{\underline{\underline{4}}}} + \tilde{\boldsymbol{\Lambda}}_{\mathrm{Q}J}^{-1\underline{\underline{2}}\underline{\underline{3}}\underline{\underline{\underline{4}}}})\boldsymbol{k}_i)\tilde{\boldsymbol{H}}_J)^{\mathrm{T}132}\tilde{\boldsymbol{H}}_K)\otimes\boldsymbol{g}^i\\
&= \mathbb{W}_{KJ}^{\mathrm{T}1324}.
\end{aligned}
\tag{17}
$$

In the expressions of Eqs. (15) and (17), we exploit for convenience of notation some dual tensors built with the differential maps of the relative rototranslations. They are the summations

$$
\begin{aligned}
&\boldsymbol{\Lambda}_{\mathrm{II}}^{-} = \sum_{J=1}^{N} W_J\tilde{\boldsymbol{\Lambda}}_J^{-1}, \quad \boldsymbol{\Lambda}_{\mathrm{II}/}^{-} = \sum_{J=1}^{N} W_{J,i}\tilde{\boldsymbol{\Lambda}}_J^{-1}\otimes\boldsymbol{g}^i,\\
&\boldsymbol{\Lambda}_{\mathrm{III}}^{-1\underline{2}\underline{3}} = \sum_{J=1}^{N} W_J\tilde{\boldsymbol{\Lambda}}_{\mathrm{III}J}^{-1\underline{2}\underline{3}}, \quad \boldsymbol{\Lambda}_{\mathrm{III}/}^{-1\underline{2}\underline{3}} = \sum_{J=1}^{N} W_{J,i}\tilde{\boldsymbol{\Lambda}}_{\mathrm{III}J}^{-1\underline{2}\underline{3}}\otimes\boldsymbol{g}^i,\\
&\boldsymbol{\Lambda}_{\mathrm{Q}}^{-1\underline{\underline{2}}\underline{\underline{3}}\underline{\underline{\underline{4}}}} = \sum_{J=1}^{N} W_J\tilde{\boldsymbol{\Lambda}}_{\mathrm{Q}J}^{-1\underline{\underline{2}}\underline{\underline{3}}\underline{\underline{\underline{4}}}};
\end{aligned}
\tag{18}
$$

the fourth-order dual tensors

$$
\begin{aligned}
\tilde{\boldsymbol{\Lambda}}_{\mathrm{L}J}^{-1\underline{2}\underline{\underline{3}}\underline{4}} &= (\tilde{\boldsymbol{\Lambda}}_{\mathrm{III}J}^{-1\underline{2}\underline{3}}\boldsymbol{I}^{\times} + \tfrac{1}{2}\tilde{\boldsymbol{\Lambda}}_J^{-1}\cdot(\boldsymbol{I}\otimes\boldsymbol{I} + (\boldsymbol{I}\otimes\boldsymbol{I})^{\mathrm{T}1342}))^{\mathrm{S}1\underline{2}\underline{\underline{3}}\underline{4}},\\
\tilde{\boldsymbol{\Lambda}}_{\mathrm{R}J}^{-1\underline{2}\underline{\underline{3}}\underline{4}} &= (\tilde{\boldsymbol{\Lambda}}_{\mathrm{III}J}^{-1\underline{2}\underline{3}}\boldsymbol{I}^{\times} + \tfrac{1}{2}\tilde{\boldsymbol{\Lambda}}_J^{-1}\cdot(\boldsymbol{I}\otimes\boldsymbol{I} + (\boldsymbol{I}\otimes\boldsymbol{I})^{\mathrm{T}1324}))^{\mathrm{S}1\underline{2}\underline{\underline{3}}\underline{4}},\\
\tilde{\boldsymbol{\Lambda}}_{\mathrm{Q}J}^{-1\underline{\underline{2}}\underline{\underline{3}}\underline{\underline{\underline{4}}}} &= \tilde{\boldsymbol{\Lambda}}_{\mathrm{IV}J}^{-1\underline{\underline{2}}\underline{\underline{3}}\underline{\underline{\underline{4}}}} - (3\tilde{\boldsymbol{\Lambda}}_{\mathrm{III}J}^{-1\underline{2}\underline{3}}\tilde{\boldsymbol{\Lambda}}_J\tilde{\boldsymbol{\Lambda}}_{\mathrm{III}J}^{-1\underline{2}\underline{3}} - \tfrac{1}{2}\tilde{\boldsymbol{\Lambda}}_J^{-1}\boldsymbol{I}^{\times}\tilde{\boldsymbol{\Lambda}}_J\tilde{\boldsymbol{\Lambda}}_{\mathrm{III}J}^{-1\underline{2}\underline{3}} + \tilde{\boldsymbol{\Lambda}}_J^{-1}\otimes\boldsymbol{I})^{\mathrm{S}1\underline{\underline{2}}\underline{\underline{3}}\underline{\underline{\underline{4}}}};
\end{aligned}
\tag{19}
$$

and the inverse form $\tilde{\boldsymbol{\Lambda}}_{J/}^{-}$ of the derivatives of the tangent map from Eqs. (B.19)$_2$,

$$
\begin{aligned}
&\tilde{\boldsymbol{\Lambda}}_{J/} = \tilde{\boldsymbol{\Lambda}}_{\mathrm{III}J}^{1\underline{2}\underline{3}} + \frac{1}{2}(\boldsymbol{I}^{\times}\tilde{\boldsymbol{\Lambda}}_J)^{\mathrm{T}132}\tilde{\boldsymbol{\Lambda}}_J,\\
&\tilde{\boldsymbol{\Lambda}}_{J/}^{-} = \tilde{\boldsymbol{\Lambda}}_{\mathrm{III}J}^{-1\underline{2}\underline{\underline{3}}} - \frac{1}{2}\tilde{\boldsymbol{\Lambda}}_J^{-1}\boldsymbol{I}^{\times},
\end{aligned}
\tag{20}
$$

which are tied by the reciprocity relations

$$
\begin{aligned}
&\tilde{\boldsymbol{\Lambda}}_{J/}^{-} = \tilde{\boldsymbol{\Lambda}}_J^{-1}((\tilde{\boldsymbol{\Lambda}}_{J/}\tilde{\boldsymbol{\Lambda}}_J^{-1})^{\mathrm{T}132}\tilde{\boldsymbol{\Lambda}}_J^{-1})^{\mathrm{T}132},\\
&\tilde{\boldsymbol{\Lambda}}_{J/} = \tilde{\boldsymbol{\Lambda}}_J((\tilde{\boldsymbol{\Lambda}}_{J/}^{-}\tilde{\boldsymbol{\Lambda}}_J)^{\mathrm{T}132}\tilde{\boldsymbol{\Lambda}}_J)^{\mathrm{T}132}.
\end{aligned}
$$

It is noted that the derivative-related tensors in Eqs. (15), (17) and (18), come in the form of dyadic compositions with the contravariant base vectors $\boldsymbol{g}^i$. The covariant component tensors are actually first computed using the known derivatives $W_{J,i}$ with respect to the domain coordinates ξ^i. In order to recover

the curvature tensor and the coefficient tensors for the differential curvatures, we need to know the base vectors, which in turn rely on the dual part of the curvature. The covariant base vectors will be computed from the curvature component vectors as $\boldsymbol{g}_i = \mathrm{dual}(\boldsymbol{X}^{\mathrm{T}}\boldsymbol{k}_i)$, see Part I. This enables building the Jacobian tensor $\boldsymbol{G} = \boldsymbol{g}_j \otimes \boldsymbol{i}^j$, with $\boldsymbol{i}^j$ the unit vectors of the absolute orthonormal base, and extracting the contravariant base vectors as the component vectors of the inverse-transpose tensor $\boldsymbol{G}^{-\mathrm{T}} = \boldsymbol{g}^j \otimes \boldsymbol{i}_j$.

5. Computational aspects

5.1. Computation of the weighted average orientation

The interpolation problem giving the weighted average orientation can be solved numerically by a sort of Newton–Raphson procedure on the vectorial equation

$$\sum_{J=1}^{N} W_J \,\mathrm{ax\,log}(\boldsymbol{\alpha}\boldsymbol{\alpha}_J^{\mathrm{T}}) = \boldsymbol{0}, \tag{21}$$

obtained extracting the axial vector of Eq. (2). In terms of relative rotations $\tilde{\boldsymbol{\Phi}}_J = \boldsymbol{\alpha}\boldsymbol{\alpha}_J^{\mathrm{T}}$ and relative rotation vectors $\tilde{\boldsymbol{\varphi}}_J = \mathrm{ax\,log}\tilde{\boldsymbol{\Phi}}_J$, Eq. (21) can be stated as $\boldsymbol{f}(\tilde{\boldsymbol{\varphi}}_J) = \boldsymbol{0}$, and in incremental form $\boldsymbol{f} + \partial\boldsymbol{f} = \boldsymbol{0}$. Let us now introduce the incremental orientation vector $\boldsymbol{y}_\partial$ such that $\boldsymbol{y}_\partial\times = \partial\boldsymbol{\alpha}\boldsymbol{\alpha}^{\mathrm{T}} = \partial\tilde{\boldsymbol{\Phi}}_J\tilde{\boldsymbol{\Phi}}_J^{\mathrm{T}} = \tilde{\boldsymbol{\varphi}}_{\partial J}\times$, and exploit the differential maps of the relative rotations, $\tilde{\boldsymbol{\varphi}}_{\partial J} = \tilde{\boldsymbol{\Gamma}}_J\,\partial\tilde{\boldsymbol{\varphi}}_J$ (see Appendix A); it follows that $\boldsymbol{y}_\partial = \tilde{\boldsymbol{\Gamma}}_J\partial\tilde{\boldsymbol{\varphi}}_J$. Therefore, the vector function $\boldsymbol{f}$ and its increment $\partial\boldsymbol{f}$ can be written

$$\begin{aligned} \boldsymbol{f} &= \sum_{J=1}^{N} W_J\tilde{\boldsymbol{\varphi}}_J, \\ \partial\boldsymbol{f} &= \sum_{J=1}^{N} W_J\tilde{\boldsymbol{\Gamma}}_J^{-1}\boldsymbol{y}_\partial. \end{aligned} \tag{22}$$

An iterative solution process can be started having vector $\boldsymbol{f}$ from Eq. $(22)_1$ as residual and using tensor $\sum W_J\tilde{\boldsymbol{\Gamma}}_J^{-1}$ from Eq. $(22)_2$ as Jacobian. At each iteration, a linear 3×3 equation set is solved for the incremental orientation vector $\boldsymbol{y}_\partial$, which is used to multiplicatively update the unknown orientation tensor, $\boldsymbol{\alpha} \leftarrow \exp(\boldsymbol{y}_\partial\times)\boldsymbol{\alpha}$.

A good starting point for this procedure is recommended, and an efficient way to achieve it is proposed here. Starting from the orientation $\boldsymbol{\alpha}_J$ with the highest associated weight, we iterate on the fictitious problem $\boldsymbol{f} + \boldsymbol{I}\boldsymbol{y}_\partial = \boldsymbol{0}$. This roughly means to regard $\sum W_J\tilde{\boldsymbol{\varphi}}_J$ as a small rotation vector to bring to zero like an error. This approaching procedure just requires the evaluation of the residual Eq. $(22)_1$ and can cheaply lower the error under 10^{-3} rad. From such a good starting point, a quadratic rate of convergence of the next procedure of the Newton–Raphson kind is practically ensured.

5.2. Computation of the weighted average oriento-position

The problem of the weighted average oriento-position, Eq. (4), could be solved numerically by the same procedure discussed above, exploiting the rules of dual algebra. However, the linear dependency of the oriento-position tensor on the position vector suggests a computationally more efficient procedure made of two steps. Extracting the axial vector of Eq. (4) and introducing the relative rototranslations $\tilde{\boldsymbol{H}}_J = \boldsymbol{A}\boldsymbol{A}_J^{\mathrm{T}}$ and the relative helices $\tilde{\boldsymbol{\eta}}_J = \mathrm{ax\,log}\tilde{\boldsymbol{H}}_J$, and exploiting Eqs. (16), (18) and $(21)_2$ from Part I, we arrive at the explicit form

$$\sum_{J=1}^{N} W_J(\tilde{\boldsymbol{\varphi}}_J + \varepsilon \tilde{\boldsymbol{\Gamma}}_J^{-1}(\boldsymbol{x} - \tilde{\boldsymbol{\Phi}}_J \boldsymbol{x}_J)) = \boldsymbol{0}. \tag{23}$$

The primal part is just Eq. (21) and is first solved for the weighted average orientation $\boldsymbol{\alpha}$. Then, the dual part reduces to a linear problem with position vector $\boldsymbol{x}$ as unknown. The interpolated oriento-position dual tensor is finally recovered as $\boldsymbol{A} = (\boldsymbol{I} + \varepsilon \boldsymbol{x}\times)\boldsymbol{\alpha}$.

5.3. Numerical validation of the interpolation formulae

The quite huge expressions of the coefficient dual tensors in Eqs. (17) have been tested numerically. Let us consider two distinct configurations, a *given* configuration and another, very close, *perturbed* configuration, and let us refer to the change of configuration as the *updating* process. Assigned values of the nodal oriento-positions define the given configuration, and an assigned set of the nodal variation variables define the updating of the nodal oriento-positions to the perturbed configuration. In both configurations, the numerical solution of Eqs. (4) and (15) yield the interpolated oriento-positions and curvatures, that we assume as 'exact'. In the given configuration, using Eqs. (14) and (16) with the assigned nodal variation variables, a set of local variation variables defining the local updating to the perturbed configuration is obtained. This local updating yields predicted oriento-positions and curvatures, which must converge to the exact values as the perturbation magnitude diminishes.

In order to test the interpolation formulae, which account for two independent variations, we need a consistent updating mechanism for oriento-positions and curvatures, which shall involve the variation variables characterizing two independent variations, say ∂ and δ. Consider a double variation that brings an oriento-position $\boldsymbol{A}$ in $\boldsymbol{A}' = \boldsymbol{A} + \delta\boldsymbol{A} + \partial(\boldsymbol{A} + \delta\boldsymbol{A}) = \boldsymbol{A} + \partial\boldsymbol{A} + \delta(\boldsymbol{A} + \partial\boldsymbol{A}) = \boldsymbol{A} + \delta\boldsymbol{A} + \partial\boldsymbol{A} + \partial\delta\boldsymbol{A}$. By applyings Eqs. (5), it follows that $\boldsymbol{A}' = (\boldsymbol{I} + \boldsymbol{a}_\delta\times + \boldsymbol{a}_\partial\times + \boldsymbol{a}_{\partial\delta}\times + \frac{1}{2}(\boldsymbol{a}_\partial\times\boldsymbol{a}_\delta\times + \boldsymbol{a}_\delta\times\boldsymbol{a}_\partial\times))\boldsymbol{A}$, and since the differential vectors $\boldsymbol{a}_\delta$, $\boldsymbol{a}_\partial$ and $\boldsymbol{a}_{\partial\delta}$ are infinitesimal, we can assume $\boldsymbol{A}' \cong (\boldsymbol{I} + \boldsymbol{a}_\delta\times + \boldsymbol{a}_\partial\times + \boldsymbol{a}_{\partial\delta}\times)\boldsymbol{A}$. Now, an infinitesimal rototranslation must transform $\boldsymbol{A}$ in $\boldsymbol{A}'$, and this condition is satisfied by substituting $\exp((\boldsymbol{a}_\delta + \boldsymbol{a}_\partial + \boldsymbol{a}_{\partial\delta})\times)$ for the transforming tensor. Similar but more involved considerations (see Merlini and Morandini, 2003) yield the transformation rule for the curvature tensor from $\boldsymbol{k}$ to $\boldsymbol{k}'$. Thus, the updating formulae for oriento-positions and curvatures are finally proposed in the form

$$\begin{aligned} \boldsymbol{A}' &= \exp(\hat{\boldsymbol{a}}_{\partial\delta}\times)\boldsymbol{A}, \\ \boldsymbol{k}' &= \operatorname{dexp}(\hat{\boldsymbol{a}}_{\partial\delta}\times)\hat{\boldsymbol{k}}_{\partial\delta} + (\boldsymbol{I} + \tfrac{1}{2}\operatorname{dexp}(\hat{\boldsymbol{a}}_{\partial\delta}\times)(\hat{\boldsymbol{a}}_{\partial\delta}\times + (\boldsymbol{a}_\delta \otimes \boldsymbol{a}_\partial)^{\mathrm{S}} + \boldsymbol{a}_\partial \cdot \boldsymbol{a}_\delta \otimes \boldsymbol{I}))\boldsymbol{k}, \end{aligned} \tag{24}$$

where

$$\begin{aligned} \hat{\boldsymbol{a}}_{\partial\delta} &= \boldsymbol{a}_\delta + \boldsymbol{a}_\partial + \boldsymbol{a}_{\partial\delta}, \\ \hat{\boldsymbol{k}}_{\partial\delta} &= \boldsymbol{k}_\delta + \boldsymbol{k}_\partial + \boldsymbol{k}_{\partial\delta}. \end{aligned}$$

In the validation tests, Eq. $(24)_1$ is also used for updating the nodal oriento-positions.

Tests are performed on four different orders of domains, described respectively by 1, 2, 3 and 4 coordinates. By using multilinear weight functions, this means elements with 2, 4, 8 and 16 nodes. The nodal oriento-positions are generated by random rototranslations of real part magnitude up to more than 2 rad, and are given random perturbations confined within a band of randomly generated width. The computations are repeated 100 times, providing a total amount of 400 different tests at disposal. The interpolation weights and their derivatives are computed each time at random internal placements.

The errors of the predicted oriento-position and curvature with respect to the exact values are measured respectively as the real part magnitude of the relative helix, and the maximum absolute difference between the scalar components of the curvatures. A quadratic rate of convergence of the interpolation formulae with decreasing the magnitude of the nodal perturbation is observed (Fig. 3), and this is a reliable evidence

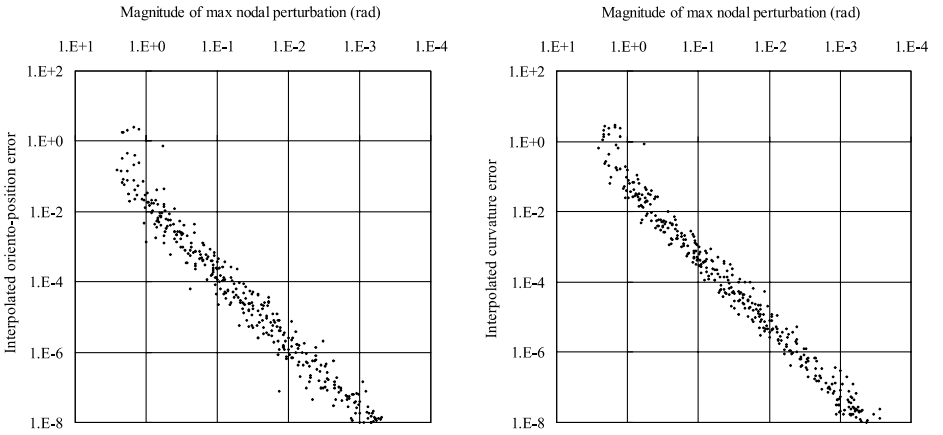

Fig. 3. Convergence of the linearization formulae of the interpolation.

of the soundness of the linearization. However, in comparison with the fairly cheap procedure yielding the interpolated oriento-position, the linearization is computationally rather expensive. The whole process is consuming a mean time of 4, 10, 34 and 141 ms per test to interpolate among 2, 4, 8 and 16 nodes respectively, on a Pentium III computer at 933 MHz.

6. Example

In this section, we discuss the description of a solid hexahedron from the position and orientation of eight corner frames. The example is taken from a finite-element simulation to be discussed in Part III, and represents the deformed configuration of an element that was initially prismatic, of size $2\times1\times1$ and aligned along the absolute axis x^1. The absolute reference frame, the deformed configuration, and a further configuration after a rigid motion, are depicted in Fig. 4 (the initial configuration is not relevant in this example). The corner data are listed in Table 1.

The model field is defined on a rectangular domain described by three material coordinate lines $\xi^i=[-1,+1]$, with ξ^1 parallel to edge 1–2, ξ^2 parallel to edge 2–3 and ξ^3 parallel to edge 1–5. Standard three-linear weight functions $W_J=\frac{1}{8}(1+\xi^1\xi^1_J)(1+\xi^2\xi^2_J)(1+\xi^3\xi^3_J)$ are used for the interpolation. Since the element edges lie on coordinate lines and the element faces lie on coordinate surfaces, the interpolation on the boundary using such weight functions is local to the boundary itself. This ensures C^0 continuity of the oriento-position field across adjacent elements. The helicoidal interpolation is exploited in this example to render the geometry of the element: each face and each edge are modeled with a number of facets and segments, and this mesh is interpolated from the corner nodes. So, faces and edges are curved surfaces and lines, respectively.

The oriento-position $\boldsymbol{A}$ of an internal frame located at $\xi=(0.2,0.0,-0.3)$ is interpolated from the eight corner frames, and the dual component vectors $\boldsymbol{k}_i$ of the curvature along the coordinate lines are computed from Eq. (15). The position $\boldsymbol{x}$, the orientation tensor $\boldsymbol{\alpha}$, the base vectors $\boldsymbol{g}_i=\mathrm{dual}(\boldsymbol{X}^{\mathrm{T}}\boldsymbol{k}_i)$ and the angular curvatures $\boldsymbol{k}_{ai}=\mathrm{primal}(\boldsymbol{X}^{\mathrm{T}}\boldsymbol{k}_i)$ are recovered and listed in Table 2. The interpolated frame and an 'elementary' volume of initial size $0.4\times0.4\times0.4$ are plotted in Fig. 4. It is easy to envisage the difference between this interpolation based on the helicoidal modeling and common interpolations based on classical uncoupled modeling. Even if the orientation would have been interpolated multiplicatively according to Eq. (2), the corner-node element built with standard isoparametric functions would have exhibited straight

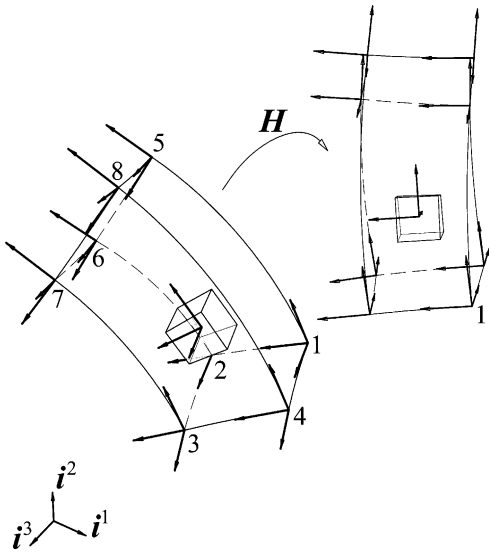

Fig. 4. Helicoidal interpolation of a deformed hexahedron.

Table 1
Positions and orientations of corner frames

	x	α_1	α_2	α_3
1	3.22989991	−0.381852659	−0.907936713	0.172741053
	4.39071471	0.906706495	−0.404230328	−0.120337749
	0.17134187	0.179086233	0.110674145	0.977588541
2	2.32012122	−0.391731346	−0.897655212	0.201895204
	3.99131867	0.895364344	−0.422436080	−0.140962585
	0.29246236	0.211823618	0.125550303	0.969209924
3	2.59481673	−0.352321916	−0.873185522	0.336773383
	3.88768434	0.914252067	−0.398036382	−0.075565848
	1.32324204	0.200031063	0.281272257	0.938548609
4	3.44536342	−0.372619388	−0.882783513	0.286091002
	4.29237833	0.909984998	−0.408019712	−0.073805264
	1.07487356	0.181884839	0.232837247	0.955355809
5	1.71236201	−0.875276697	−0.444489976	0.190576402
	5.96865365	0.464544629	−0.882307493	0.075708488
	0.50092547	0.134495324	0.154797119	0.978748619
6	1.24918588	−0.869169880	−0.420473610	0.260279972
	5.08759160	0.450635907	−0.890210064	0.066733211
	0.68019308	0.203644296	0.175293999	0.963224281
7	1.52285903	−0.837379182	−0.448146618	0.312986766
	5.24897003	0.518383601	−0.832712741	0.194596847
	1.69955113	0.173420149	0.325198555	0.929608171
8	1.93261569	−0.859252855	−0.446798858	0.249109034
	6.07401308	0.494095535	−0.851004650	0.177934507
	1.40529471	0.132492011	0.275974395	0.951989496

Table 2
Position, orientation, base vectors and angular curvatures at $\xi = (0.2, 0.0, -0.3)$ from the helicoidal interpolation, and orientation and angular curvatures from the additive interpolation (marked with an overbar)

$\boldsymbol{x}$			$\boldsymbol{\alpha}_1$	$\boldsymbol{\alpha}_2$	$\boldsymbol{\alpha}_3$	$\bar{\boldsymbol{\alpha}}_1$	$\bar{\boldsymbol{\alpha}}_2$	$\bar{\boldsymbol{\alpha}}_3$
2.46921			−0.57550633	−0.77053058	0.27399833	−0.57423280	−0.77182423	0.27302757
4.67371			0.79706182	−0.60346359	−0.02289440	0.79899357	−0.60104978	−0.01866651
0.86690			0.18298885	0.20521774	0.96145762	0.17851043	0.20742835	0.96182509
$\boldsymbol{g}_1$	$\boldsymbol{g}_2$	$\boldsymbol{g}_3$	$\boldsymbol{k}_{a1}$	$\boldsymbol{k}_{a2}$	$\boldsymbol{k}_{a3}$	$\bar{\boldsymbol{k}}_{a1}$	$\bar{\boldsymbol{k}}_{a2}$	$\bar{\boldsymbol{k}}_{a3}$
−0.38285	0.13329	−0.55683	0.00388594	−0.04595530	−0.02656145	0.00402349	−0.04615493	−0.02974501
−0.29906	−0.01282	0.77240	0.02604382	0.05505335	0.00758286	0.02622432	0.05413409	0.00781498
0.09943	0.48938	0.18416	−5.47895E−6	−0.00695709	0.33785617	−0.00023360	−0.00734615	0.33720886

Table 3
Relative rotation error and angular strain in the rigid motion by using the additive interpolation

$\bar{\boldsymbol{\varphi}}$	$\bar{\boldsymbol{\omega}}_{a1}$	$\bar{\boldsymbol{\omega}}_{a2}$	$\bar{\boldsymbol{\omega}}_{a3}$
−3.6849E−04	1.2349E−04	6.1001E−04	−6.7284E−04
−9.5707E−03	−2.9616E−04	−4.1573E−04	8.8087E−03
1.4695E−02	2.6097E−06	1.4312E−03	−7.6800E−03

edges, and the position and the shape assumed by the elementary volume would have been quite different. It can be guessed that model fields based on the helicoidal interpolation constitute a sound basis to build finite elements that do not suffer from shear-locking.

The interpolated orientation and angular curvatures are also compared in Table 2 with the outcome from the additive interpolation, Eq. (3). The orientation is computed as $\bar{\boldsymbol{\alpha}} = \exp(\bar{\boldsymbol{y}}\times)$ on the weighted average rotation vector $\bar{\boldsymbol{y}} = \sum W_J \boldsymbol{y}_J$ among those defining the nodal orientations, and the angular curvatures are computed as $\bar{\boldsymbol{k}}_{ai} = \operatorname{dexp}(\bar{\boldsymbol{y}}\times)\cdot\bar{\boldsymbol{y}}_{,i} = \operatorname{dexp}(\bar{\boldsymbol{y}}\times)\cdot\sum W_{J,i}\boldsymbol{y}_J$.

In Fig. 4, the same hexahedron is shown after a rigid rototranslation $\boldsymbol{H} = (\boldsymbol{I} + \varepsilon\boldsymbol{t}\times)\boldsymbol{\Phi}$, with translation vector $\boldsymbol{t} = 5\boldsymbol{i}^1 + 2\boldsymbol{i}^2 - 5\boldsymbol{i}^3$ and rotation vector $\boldsymbol{\varphi} = \frac{\pi}{\sqrt{69}}(\boldsymbol{i}^1 - 4\boldsymbol{i}^2 - 0.5\boldsymbol{i}^3)$. By computing new oriento-position and curvatures from the rototranslated corner frames, the helicoidal interpolation gives exactly the preceding values rototranslated, namely $\boldsymbol{A}' = \boldsymbol{H}\boldsymbol{A}$ and $\boldsymbol{k}'_i = \boldsymbol{H}\boldsymbol{k}_i$. This ensures that no strains $\boldsymbol{\omega}_i = \boldsymbol{k}'_i - \boldsymbol{H}\boldsymbol{k}_i$ arise from rigid motion, and is a numerical test for objectivity (the path independence of this interpolation example is inherent in that no history is considered). Instead, the additive interpolation gives new orientations and angular curvatures different from the preceding ones rotated by $\boldsymbol{\Phi}$, i.e. $\bar{\boldsymbol{\alpha}}' \neq \boldsymbol{\Phi}\bar{\boldsymbol{\alpha}}$ and $\bar{\boldsymbol{k}}'_{ai} \neq \boldsymbol{\Phi}\bar{\boldsymbol{k}}_{ai}$. The error is measured by the rotation vector $\bar{\boldsymbol{\varphi}}$ of the relative rotation $\bar{\boldsymbol{\alpha}}'(\boldsymbol{\Phi}\bar{\boldsymbol{\alpha}})^{\mathrm{T}}$, and the angular strains $\bar{\boldsymbol{\omega}}_{ai} = \bar{\boldsymbol{k}}'_{ai} - \boldsymbol{\Phi}\bar{\boldsymbol{k}}_{ai}$, see Table 3.

7. Conclusion

The proposed helicoidal interpolation of the oriento-position field is based on the relative rototranslations from the nodal oriento-positions. This fact ensures the consistency of the model issued by the interpolation with the underlying actual field, in the sense that the former complies with the algebraic rules of the special orthogonal manifold of rototranslations to which oriento-positions pertain. The consistency of the model leads to a genuine differentiation, which is a valuable asset in finite-element approximations of variational principles in solid mechanics. Achieving this consistency on multi-coordinate domains is a prerogative of the proposed interpolation.

The interpolation scheme is endowed with other merits. It is by nature invariant against rigid motion and frame indifferent, and at the same time path-independent. It is general as for the number of coordinates of the domain. Moreover, it is general in the sense that no definition of the weight functions has been yet attempted, so it may be applied in principle to domains of whatever shape. The implicit interpolation scheme is numerically solved by an efficient procedure, and is equipped with the parameterization-free core of a threefold consistent linearization. It is based on the helicoidal modeling of the continuum (see Part I), and constitutes the natural interpolation of the kinematical field allowing to build curved and curving finite elements based on nodal frames, capable of displacements and rotations unrestricted in size (see Part III). The proposed interpolation is guessed to play an important role in the modeling of shells in the near future.

The formulation greatly relies on the powerful formalism of dual numbers, which only makes the rototranslation differential maps available in an affordable way (Appendix B). So, the interpolation of the oriento-position is actually an extension of the interpolation of the orientation, which is also supplied in this paper and can be useful in the context of classical modeling.

A possible drawback we can pick out in this interpolation scheme is the huge expression of the coefficient tensors of the interpolation formulae. A careful investigation for obtaining simplified formulae, able to increase the computational efficiency with a minimal loss of accuracy, would be an appreciated effort.

Appendix A. The differential maps of rotation

It was shown in Part I that subsequent differentiations of the rotation are characterized each one by a new characteristic differential rotation vector. The differential vectors $\boldsymbol{\varphi}_{\delta}$, $\boldsymbol{\varphi}_{\partial\delta}$, $\boldsymbol{\varphi}_{\mathrm{d}\partial\delta}$, characterizing the differentiations up to third-order of a rotation tensor $\boldsymbol{\Phi}$, have been identified as the axial vectors of tensors $\delta\boldsymbol{\Phi}\boldsymbol{\Phi}^{\mathrm{T}}$, $\partial\delta\boldsymbol{\Phi}\boldsymbol{\Phi}^{\mathrm{T}}$ and $\mathrm{d}\partial\delta\boldsymbol{\Phi}\boldsymbol{\Phi}^{\mathrm{T}}$, respectively. The aim of this Appendix is to relate such characteristic differential rotation vectors to the variations of the rotation vector $\boldsymbol{\varphi}$, namely to establish the associated differential maps up to third-order of the exponential map of the rotation.

In spite of the rather concise results presented, the task was very complex so that the underlying work deserved a dedicated Report. Any details and related extensions can be found in Merlini (2003).

A.1. Nesting tensors

Consider an infinite family of tensor functions, defined by the following series expansions,

$$\boldsymbol{\Phi}_m = \exp_m(\boldsymbol{\varphi}\times) = \sum_{n=0}^{\infty} \frac{m!}{(n+m)!}\boldsymbol{\varphi}\times^n \quad (\forall m \geqslant 0). \tag{A.1}$$

Owing to the evident similarity with the exponential expansion, we borrow for such functions the symbolic name $\exp_m$. In particular, the first member of the family (the element zero) is just the rotation tensor, $\boldsymbol{\Phi}_0 \equiv \boldsymbol{\Phi} = \exp(\boldsymbol{\varphi}\times)$. It is a matter of elementary algebra to recognize that Eq. (A.1) can be written as

$$\boldsymbol{\Phi}_m = \sum_{n=0}^{l-1} \frac{m!}{(n+m)!}\boldsymbol{\varphi}\times^n + \frac{m!}{(l+m)!}\boldsymbol{\varphi}\times^l\boldsymbol{\Phi}_{l+m} \quad (\forall m \geqslant 0,\ \forall l > 0). \tag{A.2}$$

The meaning of Eq. (A.2) is clear: truncating the series expansion $\boldsymbol{\Phi}_m$ at the lth term is *exact*, provided that the last retained term be multiplied by a higher element of the same family, namely $\boldsymbol{\Phi}_{l+m}$. Notice that, at increasing the integer m, the elements of the family approach to the unit tensor, and at the limit $\boldsymbol{\Phi}_{\infty} = \boldsymbol{I}$.

This family of tensors establishes a new representation of the rotation tensor, which is *recursive* in the sense that the same truncation mechanism is valid for the rotation tensor itself and for each subsequent element of the family: every element can in turn be truncated at whatever term $l > 0$. In particular, consider truncating the series at the first term ($l = 1$, the strongest truncation),

$$\boldsymbol{\Phi}_m = \boldsymbol{I} + \frac{1}{m+1}\boldsymbol{\varphi}\times\boldsymbol{\Phi}_{m+1}. \tag{A.3}$$

Eq. (A.3) enables us to envisage a recursive representation of the rotation tensor $\boldsymbol{\Phi}_0$ exploiting all the elements of the infinite family. This family can be seen as a nest of tensors, so their members will be called the *nesting tensors of the rotation*.

The series expansion in Eq. (A.1) can be brought to a closed form based on two minimal tensorial bases, $\boldsymbol{\varphi}\times$ and $\boldsymbol{\varphi}\times^2$:

$$\begin{aligned}
&\boldsymbol{\Phi}_0 = \boldsymbol{I} + a\boldsymbol{\varphi}\times + b_0\boldsymbol{\varphi}\times^2,\\
&\boldsymbol{\Phi}_1 = \boldsymbol{I} + b_0\boldsymbol{\varphi}\times + b_1\boldsymbol{\varphi}\times^2,\\
&\boldsymbol{\Phi}_m = \boldsymbol{I} + mb_{m-1}\boldsymbol{\varphi}\times + b_m\boldsymbol{\varphi}\times^2 \quad (\forall m \geqslant 1).
\end{aligned} \tag{A.4}$$

Eqs. (A.4) are referred to as the *short forms* of the nesting tensors, and are of much interest for computational purposes. They are drawn using the recurrence formula $\boldsymbol{\varphi}\times^3 + \varphi^2\boldsymbol{\varphi}\times = \boldsymbol{0}$, with φ the rotation angle, and exploit a recursive series of coefficient functions,

$$\begin{aligned}
a &= \sum_{n=0}^{\infty} \tfrac{(-1)^n}{(2n+1)!}\varphi^{2n} && = \tfrac{1}{\varphi}\sin\varphi,\\
b_0 &= 0!\sum_{n=0}^{\infty} \tfrac{(-1)^n}{(2n+2)!}\varphi^{2n} && = \tfrac{1}{\varphi^2}(1-\cos\varphi),\\
b_1 &= 1!\sum_{n=0}^{\infty} \tfrac{(-1)^n}{(2n+3)!}\varphi^{2n} && = \tfrac{1}{\varphi^2}(1-a),\\
b_m &= m!\sum_{n=0}^{\infty} \tfrac{(-1)^n}{(2n+2+m)!}\varphi^{2n} \quad (\forall m \geqslant 0) && = \tfrac{1}{\varphi^2}(1-m(m-1)\,b_{m-2}) \quad (\forall m \geqslant 2).
\end{aligned} \tag{A.5}$$

The coefficient functions in Eqs. (A.5) can be computed by truncated series expansions from the left column at small angles, and by the analytical formulae from the right column at angles far enough off the singularity point. Unfortunately, the numerical ill-conditioning of the recursive analytical formulae is growing with the coefficient index; so, the threshold angles for switching from the series to the analytical expressions become quite large for high coefficients. This in turn demands a higher truncation term of the series expansion in order to preserve accuracy. For the lowest twelve coefficient functions, a fairly good accuracy of 1.E–15 in double precision floating point was achieved on a Pentium processor by keeping to the parameters from Table 4. The accuracy was checked against 'exact' values computed in an arbitrary precision software environment (Ring, 2003).

The nesting tensors are endowed with several remarkable properties. For instance, they share the eigenvector $\boldsymbol{\varphi}$; they commute with $\boldsymbol{\varphi}\times$, $\boldsymbol{\Phi}_m\boldsymbol{\varphi}\times = \boldsymbol{\varphi}\times\boldsymbol{\Phi}_m$; they commute with each other, $\boldsymbol{\Phi}_m\boldsymbol{\Phi}_n = \boldsymbol{\Phi}_n\boldsymbol{\Phi}_m$; a useful relation between two subsequent nesting tensors follows from Eq. (A.3), written as $\boldsymbol{\varphi}\times\boldsymbol{\Phi}_m = m(\boldsymbol{\Phi}_{m-1} - \boldsymbol{I})$, in the forms

$$\begin{aligned}
&\boldsymbol{\Phi}_m - \boldsymbol{\Phi}_{m+1} = \frac{1}{(m+1)(m+2)}((m+2)\boldsymbol{\Phi}_{m+1} - (m+1)\boldsymbol{\Phi}_{m+2})\boldsymbol{\varphi}\times \quad (\forall m \geqslant 0),\\
&(\boldsymbol{\Phi}_m - \boldsymbol{\Phi}_{m+1})\boldsymbol{\varphi}\times = \boldsymbol{I} + m\boldsymbol{\Phi}_{m-1} - (m+1)\boldsymbol{\Phi}_m \quad (\forall m \geqslant 1);
\end{aligned}$$

the transpose nesting tensors are made of the opposite rotation, $\boldsymbol{\Phi}_m^{\mathrm{T}} = \exp_m(-\boldsymbol{\varphi}\times)$; the transpose and inverse forms are tied by the relations

$$\begin{aligned}
&\boldsymbol{\Phi}_m = \boldsymbol{I} - (\det\boldsymbol{\Phi}_m)\boldsymbol{\Phi}_m^{-\mathrm{T}}(\boldsymbol{\Phi}_m^{-1} - \boldsymbol{I}) \quad \boldsymbol{\Phi}_m^{-1} = \boldsymbol{I} - (\det\boldsymbol{\Phi}_m)^{-1}\boldsymbol{\Phi}_m^{\mathrm{T}}(\boldsymbol{\Phi}_m - \boldsymbol{I}),\\
&\boldsymbol{\Phi}_m^{\mathrm{T}} = \boldsymbol{I} - (\det\boldsymbol{\Phi}_m)(\boldsymbol{\Phi}_m^{-\mathrm{T}} - \boldsymbol{I})\boldsymbol{\Phi}_m^{-1} \quad \boldsymbol{\Phi}_m^{-\mathrm{T}} = \boldsymbol{I} - (\det\boldsymbol{\Phi}_m)^{-1}(\boldsymbol{\Phi}_m^{\mathrm{T}} - \boldsymbol{I})\boldsymbol{\Phi}_m.
\end{aligned}$$

Other properties useful for the derivations to follow can be found in Merlini (2003).

Table 4
Recursive coefficient functions. Threshold angles for switching from series to analytical expressions and truncation term in the series expansion

Coefficient function	Threshold angle (rad)	Truncation term
a	1.E–8	0
b_0	0.015	2
b_1	0.5	5
b_2	1.2	7
b_3	1.4	7
b_4	2.1	8
b_5	2.3	8
b_6	2.6	8
b_7	2.7	8
b_8	3.6	9
b_9	4.0	9
b_{10}	4.2	9

A.2. Derivatives of the nesting tensors

By taking a single variation δ and a double variation $\partial\delta$ of the nesting tensors,

$$\begin{aligned}\delta\boldsymbol{\Phi}_m &= \boldsymbol{\Phi}_{m/} : \delta\boldsymbol{\varphi} \otimes \boldsymbol{I},\\ \partial\delta\boldsymbol{\Phi}_m &= \boldsymbol{\Phi}_{m/} : \partial\delta\boldsymbol{\varphi} \otimes \boldsymbol{I} + \boldsymbol{\Phi}^{1\underline{2}\underline{3}4}_{m//} : \partial\boldsymbol{\varphi} \otimes \delta\boldsymbol{\varphi} \otimes \boldsymbol{I},\end{aligned} \tag{A.6}$$

the relevant first and second derivatives with respect to the rotation vector become identified as the third-order and fourth-order tensors $\boldsymbol{\Phi}_{m/}$ and $\boldsymbol{\Phi}^{1\underline{2}\underline{3}4}_{m//}$, respectively. The latter is of course endowed with symmetry of the inner component vectors, since differentiations commute. This symmetry is marked by the notation $(\ )^{1\underline{2}\underline{3}4}$, where the positions 2 and 3 of the component vectors are underlined. From Eqs. (A.6), the differentiation formula of the first derivative tensor is immediate,

$$\delta\boldsymbol{\Phi}_{m/} = \boldsymbol{\Phi}^{1\underline{2}\underline{3}4}_{m//} : \delta\boldsymbol{\varphi} \otimes \boldsymbol{I}. \tag{A.7}$$

On differentiation of functions $\exp_m$ from Eq. (A.1) by the formula

$$\delta\exp_m(\boldsymbol{\varphi}\times) = \sum_{n=0}^{\infty}\sum_{l=0}^{\infty}\frac{m!}{(n+l+1+m)!}\boldsymbol{\varphi}\times^n\delta\boldsymbol{\varphi}\times\boldsymbol{\varphi}\times^l, \tag{A.8}$$

the evaluation of Eqs. (A.6) yields concise expressions for the *first* and *second derivative tensors* of the nesting tensors:

$$\begin{aligned}\boldsymbol{\Phi}_{m/} &= -\frac{1}{2(m+1)}\left(\boldsymbol{I}^{\times}(2\boldsymbol{\Phi}_{m+1}-\boldsymbol{I}) + (2\boldsymbol{\Phi}_{m+1}-\boldsymbol{I})\boldsymbol{I}^{\times} + \boldsymbol{\varphi}\times\boldsymbol{I}^{\times}(\boldsymbol{\Phi}_{m+1}-\boldsymbol{\Phi}_{m+2}) + (\boldsymbol{\Phi}_{m+1}-\boldsymbol{\Phi}_{m+2})\boldsymbol{I}^{\times}\boldsymbol{\varphi}\times\right),\\ \boldsymbol{\Phi}^{1\underline{2}\underline{3}4}_{m//} &= -\frac{1}{2(m+1)}\left(2\boldsymbol{I}^{\times}\boldsymbol{\Phi}_{m+1/} + 2\boldsymbol{\Phi}_{m+1/}\boldsymbol{I}^{\times} + \boldsymbol{\varphi}\times\boldsymbol{I}^{\times}(\boldsymbol{\Phi}_{m+1/}-\boldsymbol{\Phi}_{m+2/}) + (\boldsymbol{\Phi}_{m+1/}-\boldsymbol{\Phi}_{m+2/})\boldsymbol{I}^{\times}\boldsymbol{\varphi}\times\right.\\ &\quad \left. - \boldsymbol{I}^{\times}\boldsymbol{I}^{\times}(\boldsymbol{\Phi}_{m+1}-\boldsymbol{\Phi}_{m+2}) - (\boldsymbol{\Phi}_{m+1}-\boldsymbol{\Phi}_{m+2})\boldsymbol{I}^{\times}\boldsymbol{I}^{\times}\right)^{\mathrm{S}1\underline{2}\underline{3}4}.\end{aligned} \tag{A.9}$$

It is worth noting that the derivative tensors are recursively built with the lower-order derivatives of the two next nesting tensors. In Eqs. (A.9), $\boldsymbol{I}^{\times} = \boldsymbol{g}_j\times\otimes\boldsymbol{g}^j$ is the third-order Ricci's tensor. The notation $(\ )^{\mathrm{S}1\underline{2}\underline{3}4}$ stands for the symmetric part of a fourth-order tensor with respect to the inner component vectors.

A.3. Rotation differential maps up to third-order

The differential rotation vectors $\boldsymbol{\varphi}_\delta$, $\boldsymbol{\varphi}_{\partial\delta}$, $\boldsymbol{\varphi}_{\mathrm{d}\partial\delta}$, characterizing the differentiations up to third-order of the rotation tensor $\boldsymbol{\Phi}$, have been defined (Merlini, 2002) as the axial vectors of the following tensors, respectively,

$$\begin{aligned}
&\delta\boldsymbol{\Phi}\,\boldsymbol{\Phi}^{\mathrm{T}} = \boldsymbol{\varphi}_\delta\times,\\
&\partial\delta\boldsymbol{\Phi}\,\boldsymbol{\Phi}^{\mathrm{T}} = \boldsymbol{\varphi}_{\partial\delta}\times + \frac{1}{2}(\boldsymbol{\varphi}_\partial\times\boldsymbol{\varphi}_\delta\times + \boldsymbol{\varphi}_\delta\times\boldsymbol{\varphi}_\partial\times),\\
&\mathrm{d}\partial\delta\boldsymbol{\Phi}\,\boldsymbol{\Phi}^{\mathrm{T}} = \boldsymbol{\varphi}_{\mathrm{d}\partial\delta}\times + \frac{1}{2}(\boldsymbol{\varphi}_{\mathrm{d}\partial}\times\boldsymbol{\varphi}_\delta\times + \boldsymbol{\varphi}_{\partial\delta}\times\boldsymbol{\varphi}_\mathrm{d}\times + \boldsymbol{\varphi}_{\delta\mathrm{d}}\times\boldsymbol{\varphi}_\partial\times + \boldsymbol{\varphi}_\mathrm{d}\times\boldsymbol{\varphi}_{\partial\delta}\times + \boldsymbol{\varphi}_\partial\times\boldsymbol{\varphi}_{\delta\mathrm{d}}\times + \boldsymbol{\varphi}_\delta\times\boldsymbol{\varphi}_{\mathrm{d}\partial}\times).
\end{aligned} \tag{A.10}$$

From Eqs. (A.10), by exploiting the recursive representation by means of nesting tensors, and the relevant differentiation formulae Eqs. (A.6), the differential rotation vectors can be brought to the following forms,

$$\begin{aligned}
&\boldsymbol{\varphi}_\delta = \boldsymbol{\Gamma}\,\delta\boldsymbol{\varphi},\\
&\boldsymbol{\varphi}_{\partial\delta} = \boldsymbol{\Gamma}\,\partial\delta\boldsymbol{\varphi} + \boldsymbol{\Gamma}_{\mathrm{III}}^{1\underline{2}\underline{3}} : \partial\boldsymbol{\varphi}\otimes\delta\boldsymbol{\varphi},\\
&\boldsymbol{\varphi}_{\mathrm{d}\partial\delta} = \boldsymbol{\Gamma}\mathrm{d}\partial\delta\boldsymbol{\varphi} + \boldsymbol{\Gamma}_{\mathrm{III}}^{1\underline{2}\underline{3}} : (\mathrm{d}\boldsymbol{\varphi}\otimes\partial\delta\boldsymbol{\varphi} + \partial\boldsymbol{\varphi}\otimes\delta\mathrm{d}\boldsymbol{\varphi} + \delta\boldsymbol{\varphi}\otimes\mathrm{d}\partial\boldsymbol{\varphi})\\
&\qquad + \left(\boldsymbol{\Gamma}_{\mathrm{IV}}^{1\underline{\underline{2}}\underline{\underline{3}}4} - \left(\frac{1}{2}(\boldsymbol{\Gamma}^\times\boldsymbol{\Gamma})^{\mathrm{T}132}\boldsymbol{\Gamma}_{\mathrm{III}}^{1\underline{2}\underline{3}} + \boldsymbol{\Gamma}\otimes\boldsymbol{\Gamma}^{\mathrm{T}}\boldsymbol{\Gamma}\right)^{\mathrm{S}1\underline{\underline{2}}\underline{\underline{3}}4}\right) \vdots\ \mathrm{d}\boldsymbol{\varphi}\otimes\partial\boldsymbol{\varphi}\otimes\delta\boldsymbol{\varphi},
\end{aligned} \tag{A.11}$$

that can be inverted for

$$\begin{aligned}
&\delta\boldsymbol{\varphi} = \boldsymbol{\Gamma}^{-1}\boldsymbol{\varphi}_\delta,\\
&\partial\delta\boldsymbol{\varphi} = \boldsymbol{\Gamma}^{-1}\boldsymbol{\varphi}_{\partial\delta} - \boldsymbol{\Gamma}_{\mathrm{III}}^{-1\underline{2}\underline{3}} : \boldsymbol{\varphi}_\partial\otimes\boldsymbol{\varphi}_\delta,\\
&\mathrm{d}\partial\delta\boldsymbol{\varphi} = \boldsymbol{\Gamma}^{-1}\boldsymbol{\varphi}_{\mathrm{d}\partial\delta} - \boldsymbol{\Gamma}_{\mathrm{III}}^{-1\underline{2}\underline{3}} : (\boldsymbol{\varphi}_\mathrm{d}\otimes\boldsymbol{\varphi}_{\partial\delta} + \boldsymbol{\varphi}_\partial\otimes\boldsymbol{\varphi}_{\delta\mathrm{d}} + \boldsymbol{\varphi}_\delta\otimes\boldsymbol{\varphi}_{\mathrm{d}\partial})\\
&\qquad - \left(\boldsymbol{\Gamma}_{\mathrm{IV}}^{-1\underline{\underline{2}}\underline{\underline{3}}4} - \left(3\boldsymbol{\Gamma}_{\mathrm{III}}^{-1\underline{2}\underline{3}}\boldsymbol{\Gamma}\boldsymbol{\Gamma}_{\mathrm{III}}^{-1\underline{2}\underline{3}} - \frac{1}{2}\boldsymbol{\Gamma}^{-1}\boldsymbol{\Gamma}^\times\boldsymbol{\Gamma}\boldsymbol{\Gamma}_{\mathrm{III}}^{-1\underline{2}\underline{3}} + \boldsymbol{\Gamma}^{-1}\otimes\boldsymbol{\Gamma}\right)^{\mathrm{S}1\underline{\underline{2}}\underline{\underline{3}}4}\right) \vdots\ \boldsymbol{\varphi}_\mathrm{d}\otimes\boldsymbol{\varphi}_\partial\otimes\boldsymbol{\varphi}_\delta.
\end{aligned} \tag{A.12}$$

Eqs. (A.11) constitute the associated *differential maps*, up to third-order, of the exponential map of the rotation. The mapping $\delta\boldsymbol{\varphi}\to\boldsymbol{\varphi}_\delta$ stated by Eq. $(A.11)_1$ is well known in the literature on finite rotations and represents the tangent map (or first differential map) of rotation (e.g. Cardona and Geradin, 1988; Ibrahimbegović et al., 1995; Borri and Bottasso, 1998; Borri et al., 2000; Ritto-Corrêa and Camotim, 2002; Bauchau and Trainelli, 2003). As for the notation, forms like $(\ )^{\mathrm{T}abc}$ and $(\ )^{\mathrm{T}abcd}$ specify the transpose of a third-order or a fourth-order tensor, respectively, by indicating the ordering of the component vectors in the dyadic representation; for instance, $(\ )^{\mathrm{T}132}$ transposes the two component vectors on the right, and $(\ )^{\mathrm{T}1324}$ transposes the two component vectors in the middle. The symmetric part of a tensor is denoted by $(\ )^{\mathrm{S}abc}$ or $(\ )^{\mathrm{S}abcd}$, where the positions of the two symmetric component vectors are underlined; in particular, a double underlining as in $(\ )^{\mathrm{S}1\underline{\underline{2}}\underline{\underline{3}}4}$ stands for the full-symmetric part of a fourth-order tensor with respect to the three component vectors on the right, which is defined as $(\ )^{\mathrm{S}1\underline{\underline{2}}\underline{\underline{3}}4} = \frac{1}{6}((\ ) + (\ )^{\mathrm{T}1324} + (\ )^{\mathrm{T}1243} + (\ )^{\mathrm{T}1432} + (\ )^{\mathrm{T}1342} + (\ )^{\mathrm{T}1423})$. Finally, $(\ )^{1\underline{2}\underline{3}}$ denotes a third-order symmetric tensor with respect to the two component vectors on the right, and $(\ )^{1\underline{\underline{2}}\underline{\underline{3}}4}$ denotes a fourth-order full-symmetric tensor with respect to the three component vectors on the right.

The direct forms of the mapping tensors in Eqs. (A.11) are strictly related to the first nesting tensor and to the relevant first and second derivative tensors,

$$\begin{aligned}
&\boldsymbol{\Gamma} = \boldsymbol{\Phi}_1,\\
&\boldsymbol{\Gamma}_{\mathrm{III}}^{1\underline{2}\underline{\underline{3}}} = \boldsymbol{\Phi}_{1/}^{\mathrm{S}1\underline{2}\underline{\underline{3}}},\\
&\boldsymbol{\Gamma}_{\mathrm{IV}}^{1\underline{\underline{2}}\underline{\underline{\underline{3}}}4} = \boldsymbol{\Phi}_{1//}^{1\underline{2}\underline{\underline{3}}4\mathrm{S}1\underline{\underline{2}}\underline{\underline{\underline{3}}}4}.
\end{aligned} \tag{A.13}$$

Tensors $\boldsymbol{\Gamma}^{-1}$, $\boldsymbol{\Gamma}_{\mathrm{III}}^{-1\underline{2}\underline{\underline{3}}}$, $\boldsymbol{\Gamma}_{\mathrm{IV}}^{-1\underline{\underline{2}}\underline{\underline{\underline{3}}}4}$ in Eqs. (A.12) represent the inverse forms of the mapping tensors. The direct and inverse forms are tied by the reciprocity relations

$$\begin{aligned}
&\boldsymbol{\Gamma}_{\mathrm{III}}^{-1\underline{2}\underline{\underline{3}}} = \boldsymbol{\Gamma}^{-1}(\boldsymbol{\Gamma}_{\mathrm{III}}^{1\underline{2}\underline{\underline{3}}}\boldsymbol{\Gamma}^{-1})^{\mathrm{T}132}\boldsymbol{\Gamma}^{-1},\\
&\boldsymbol{\Gamma}_{\mathrm{III}}^{1\underline{2}\underline{\underline{3}}} = \boldsymbol{\Gamma}(\boldsymbol{\Gamma}_{\mathrm{III}}^{-1\underline{2}\underline{\underline{3}}}\boldsymbol{\Gamma})^{\mathrm{T}132}\boldsymbol{\Gamma},\\
&\boldsymbol{\Gamma}_{\mathrm{IV}}^{-1\underline{2}\underline{\underline{3}}4} = \boldsymbol{\Gamma}^{-1}((\boldsymbol{\Gamma}_{\mathrm{IV}}^{1\underline{2}\underline{\underline{3}}4}\boldsymbol{\Gamma}^{-1})^{\mathrm{T}1423}\boldsymbol{\Gamma}^{-1})^{\mathrm{T}1423}\boldsymbol{\Gamma}^{-1},\\
&\boldsymbol{\Gamma}_{\mathrm{IV}}^{1\underline{2}\underline{\underline{3}}4} = \boldsymbol{\Gamma}((\boldsymbol{\Gamma}_{\mathrm{IV}}^{-1\underline{2}\underline{\underline{3}}4}\boldsymbol{\Gamma})^{\mathrm{T}1423}\boldsymbol{\Gamma})^{\mathrm{T}1423}\boldsymbol{\Gamma}.
\end{aligned} \tag{A.14}$$

A.4. Derivatives of the rotation exponential and tangent maps

For the sake of completeness and for future reference, we give the expressions of the derivatives of the exponential and tangent maps of the rotation, namely tensors $\boldsymbol{\Phi} \equiv \boldsymbol{\Phi}_0$ and $\boldsymbol{\Gamma} \equiv \boldsymbol{\Phi}_1$. According to the differentiation formulae

$$\begin{aligned}
&\delta\boldsymbol{\Phi} = \boldsymbol{\Phi}_{/} : \delta\boldsymbol{\varphi} \otimes \boldsymbol{I},\\
&\delta\boldsymbol{\Gamma} = \boldsymbol{\Gamma}_{/} : \delta\boldsymbol{\varphi} \otimes \boldsymbol{I},
\end{aligned} \tag{A.15}$$

the derivative tensors become identified by the third-order tensors

$$\begin{aligned}
&\boldsymbol{\Phi}_{/} \equiv \boldsymbol{\Phi}_{0/} = (\boldsymbol{\Phi}\boldsymbol{I}^{\times}\boldsymbol{\Gamma}^{\mathrm{T}})^{\mathrm{T}132},\\
&\boldsymbol{\Gamma}_{/} \equiv \boldsymbol{\Phi}_{1/} = \boldsymbol{\Gamma}_{\mathrm{III}}^{1\underline{2}\underline{3}} + \frac{1}{2}(\boldsymbol{I}^{\times}\boldsymbol{\Gamma})^{\mathrm{T}132}\boldsymbol{\Gamma}.
\end{aligned} \tag{A.16}$$

The variations of such derivative tensors,

$$\begin{aligned}
&\delta\boldsymbol{\Phi}_{/} = \boldsymbol{\Phi}_{//}^{1\underline{2}\underline{\underline{3}}4} : \delta\boldsymbol{\varphi} \otimes \boldsymbol{I},\\
&\delta\boldsymbol{\Gamma}_{/} = \boldsymbol{\Gamma}_{//}^{1\underline{2}\underline{\underline{3}}4} : \delta\boldsymbol{\varphi} \otimes \boldsymbol{I},
\end{aligned} \tag{A.17}$$

identify the second derivative tensors $\boldsymbol{\Phi}_{//}^{1\underline{2}\underline{\underline{3}}4} \equiv \boldsymbol{\Phi}_{0//}^{1\underline{2}\underline{\underline{3}}4}$ and $\boldsymbol{\Gamma}_{//}^{1\underline{2}\underline{\underline{3}}4} \equiv \boldsymbol{\Phi}_{1//}^{1\underline{2}\underline{\underline{3}}4}$, cf. Eq. (A.7).

Appendix B. The differential maps of rototranslation

Establishing the associated differential maps of the exponential map of the rototranslation is a plain extension of the formulation drawn in Appendix A, owing to the properties of the algebra of dual numbers applied to dual tensors. In this Appendix, we give the relations between the differential helices characterizing differentiations up to third-order of a rototranslation tensor and the variations of the helix itself. Meanwhile, we point out some noteworthy explicit expressions, as the dual parts of the quantities involved are closely related with appropriate quantities of the case of rotation. In particular, it will be seen that they always appear as one-order higher derivatives. It should be noted that an explicit formulation of the differential maps of the rototranslation would have been very much harder. Details and extensions can be found in Merlini (2003).

B.1. Dual nesting tensors

The infinite family of dual *nesting tensors of the rototranslation* is defined the same way as for the case of rotation by the series expansions

$$\boldsymbol{H}_m = \exp_m(\boldsymbol{\eta}\times) = \sum_{n=0}^{\infty} \frac{m!}{(n+m)!}\,\boldsymbol{\eta}\times^n \quad (\forall m \geqslant 0). \tag{B.1}$$

Again, the element zero coincides with the rototranslation dual tensor, $\boldsymbol{H}_0 \equiv \boldsymbol{H} = \exp(\boldsymbol{\eta}\times)$, with $\boldsymbol{\eta}$ the helix. The recursive truncation mechanism operated by tensors $\boldsymbol{H}_m$ is evident from the relation

$$\boldsymbol{H}_m = \sum_{n=0}^{l-1} \frac{m!}{(n+m)!}\,\boldsymbol{\eta}\times^n + \frac{m!}{(l+m)!}\boldsymbol{\eta}\times^l \boldsymbol{H}_{l+m} \quad (\forall m \geqslant 0,\ \forall l > 0), \tag{B.2}$$

which reduces to the strongest truncation for $l = 1$,

$$\boldsymbol{H}_m = \boldsymbol{I} + \frac{1}{m+1}\boldsymbol{\eta}\times\boldsymbol{H}_{m+1}. \tag{B.3}$$

By using the helix explicit expression $\boldsymbol{\eta} = \boldsymbol{\varphi} + \varepsilon\boldsymbol{\rho}$ in the series expansions of Eq. (B.1), the following explicit formula is obtained,

$$\exp_m(\boldsymbol{\eta}\times) = \exp_m(\boldsymbol{\varphi}\times) + \varepsilon \sum_{n=0}^{\infty}\sum_{l=0}^{\infty} \frac{m!}{(n+l+1+m)!}\,\boldsymbol{\varphi}\times^n \boldsymbol{\rho}\times\boldsymbol{\varphi}\times^l, \tag{B.4}$$

having a dual part linear with $\boldsymbol{\rho}$ and worth comparing with Eq. (A.8). Thus, by recalling Eq. $(A.6)_1$, the dual nesting tensors are found to possess the explicit expression

$$\boldsymbol{H}_m = \boldsymbol{\Phi}_m + \varepsilon\,\boldsymbol{\Phi}_{m/} : \boldsymbol{\rho} \otimes \boldsymbol{I}, \tag{B.5}$$

built with the corresponding nesting tensors of the rotation and their first derivative tensors. The dual part of Eq. (B.5) is linear with vector $\boldsymbol{\rho}$ and worth comparing with Eq. $(A.6)_1$.

The nesting tensors of rototranslation are endowed with all the properties of the nesting tensors of rotation. In particular, the short forms based on two minimal dual-tensorial bases $\boldsymbol{\eta}\times$ and $\boldsymbol{\eta}\times^2$ are given,

$$\begin{aligned} \boldsymbol{H}_0 &= \boldsymbol{I} + A\boldsymbol{\eta}\times + B_0\boldsymbol{\eta}\times^2, \\ \boldsymbol{H}_1 &= \boldsymbol{I} + B_0\boldsymbol{\eta}\times + B_1\boldsymbol{\eta}\times^2, \\ \boldsymbol{H}_m &= \boldsymbol{I} + mB_{m-1}\boldsymbol{\eta}\times + B_m\boldsymbol{\eta}\times^2 \quad (\forall m \geqslant 1), \end{aligned} \tag{B.6}$$

being used for numerical evaluations. They are obtained by the recurrence formula $\boldsymbol{\eta}\times^3 + \eta^2\boldsymbol{\eta}\times = \boldsymbol{0}$ (with η the helix dual magnitude) and exploit the recursive series of dual coefficient functions

$$\begin{aligned} A &= \sum_{n=0}^{\infty} \frac{(-1)^n}{(2n+1)!}\eta^{2n} && = \frac{1}{\eta}\sin\eta, \\ B_0 &= 0!\sum_{n=0}^{\infty} \frac{(-1)^n}{(2n+2)!}\eta^{2n} && = \frac{1}{\eta^2}(1-\cos\eta), \\ B_1 &= 1!\sum_{n=0}^{\infty} \frac{(-1)^n}{(2n+3)!}\eta^{2n} && = \frac{1}{\eta^2}(1-A), \\ B_m &= m!\sum_{n=0}^{\infty} \frac{(-1)^n}{(2n+2+m)!}\eta^{2n} \quad (\forall m \geqslant 0) && = \frac{1}{\eta^2}(1-m(m-1)B_{m-2}) \quad (\forall m \geqslant 2) \end{aligned} \tag{B.7}$$

Such coefficients allow also the following recursive explicit expressions,

$$A = a + \varepsilon\,(b_1 - b_0)\varphi\rho,$$
$$B_m = b_m + \varepsilon\,\frac{1}{m+1}(b_{m+2} - b_{m+1})\varphi\rho \quad (\forall m \geqslant 0), \tag{B.8}$$

the dual parts of which are once again linear with the helix dual part magnitude ρ. Although Eqs. (B.8) could be used to build the dual coefficient functions from Eqs. (A.5), the direct computation from the series and analytical expressions of Eqs. (B.7) is preferred. However, Eqs. (B.8) suggest that the threshold values in Table 4 should be increased for the dual case; in practice, it is found that just the coefficients A and B_0 are affected. For such coefficients, we propose to raise the threshold values to 0.001 and 0.1 (and the truncation terms to 2 and 4), respectively, being satisfied with an accuracy of 1.E–13 for the dual parts. For all the dual coefficients, the helix primal part magnitude φ can be tested against the threshold real value.

B.2. Derivatives of the dual nesting tensors

The differentiation formulae

$$\delta\boldsymbol{H}_m = \boldsymbol{H}_{m/} : \delta\boldsymbol{\eta} \otimes \boldsymbol{I},$$
$$\partial\delta\boldsymbol{H}_m = \boldsymbol{H}_{m/} : \partial\delta\boldsymbol{\eta} \otimes \boldsymbol{I} + \boldsymbol{H}^{12\underline{2}34}_{m//} \vdots \partial\boldsymbol{\eta} \otimes \delta\boldsymbol{\eta} \otimes \boldsymbol{I}, \tag{B.9}$$

enable identifying the first and second derivatives of the dual nesting tensors with respect to the helix, as the third-order and fourth-order dual tensors $\boldsymbol{H}_{m/}$ and $\boldsymbol{H}^{12\underline{2}34}_{m//}$, respectively. It also follows the differentiation formula of the first derivative dual tensor,

$$\delta\boldsymbol{H}_{m/} = \boldsymbol{H}^{12\underline{2}34}_{m//} : \delta\boldsymbol{\eta} \otimes \boldsymbol{I}. \tag{B.10}$$

The extension of Eqs. (A.9) to the first and second derivative tensors of the dual nesting tensors is straightforward, and yields

$$\boldsymbol{H}_{m/} = -\frac{1}{2(m+1)}(\boldsymbol{I}^{\times}(2\boldsymbol{H}_{m+1} - \boldsymbol{I}) + (2\boldsymbol{H}_{m+1} - \boldsymbol{I})\boldsymbol{I}^{\times} + \boldsymbol{\eta}\times\boldsymbol{I}^{\times}(\boldsymbol{H}_{m+1} - \boldsymbol{H}_{m+2}) + (\boldsymbol{H}_{m+1} - \boldsymbol{H}_{m+2})\boldsymbol{I}^{\times}\boldsymbol{\eta}\times),$$
$$\begin{aligned}\boldsymbol{H}^{12\underline{2}34}_{m//} = -\frac{1}{2(m+1)}&(2\boldsymbol{I}^{\times}\boldsymbol{H}_{m+1/} + 2\boldsymbol{H}_{m+1/}\boldsymbol{I}^{\times} + \boldsymbol{\eta}\times\boldsymbol{I}^{\times}(\boldsymbol{H}_{m+1/} - \boldsymbol{H}_{m+2/}) + (\boldsymbol{H}_{m+1/} - \boldsymbol{H}_{m+2/})\boldsymbol{I}^{\times}\boldsymbol{\eta}\times \\ &- \boldsymbol{I}^{\times}\boldsymbol{I}^{\times}(\boldsymbol{H}_{m+1} - \boldsymbol{H}_{m+2}) - (\boldsymbol{H}_{m+1} - \boldsymbol{H}_{m+2})\boldsymbol{I}^{\times}\boldsymbol{I}^{\times})^{\mathrm{S}12\underline{2}34}.\end{aligned} \tag{B.11}$$

For the first derivative of the dual nesting tensors, the explicit expression is easily drawn by recalling Eqs. (B.5), $(A.6)_1$ and (A.7),

$$\boldsymbol{H}_{m/} = \boldsymbol{\Phi}_{m/} + \varepsilon\boldsymbol{\Phi}^{12\underline{2}34}_{m//} : \boldsymbol{\rho} \otimes \boldsymbol{I}. \tag{B.12}$$

It is built with the first and second derivative of the corresponding nesting tensors of the rotation. The dual part of Eq. (B.12) is linear with vector $\boldsymbol{\rho}$ and worth comparing with Eq. (A.7).

B.3. Rototranslation differential maps up to third-order

From the definition of the differential helices $\boldsymbol{\eta}_{\delta}$, $\boldsymbol{\eta}_{\partial\delta}$, $\boldsymbol{\eta}_{\mathrm{d}\partial\delta}$, characterizing the differentiations up to third-order of a rototranslation tensor $\boldsymbol{H}$ (Merlini, 2002),

$$\begin{aligned}
&\delta \boldsymbol{H}\boldsymbol{H}^{\mathrm{T}} = \boldsymbol{\eta}_{\delta}\times,\\
&\partial\delta \boldsymbol{H}\boldsymbol{H}^{\mathrm{T}} = \boldsymbol{\eta}_{\partial\delta}\times + \frac{1}{2}(\boldsymbol{\eta}_{\partial}\times\boldsymbol{\eta}_{\delta}\times + \boldsymbol{\eta}_{\delta}\times\boldsymbol{\eta}_{\partial}\times),\\
&\mathrm{d}\partial\delta \boldsymbol{H}\boldsymbol{H}^{\mathrm{T}} = \boldsymbol{\eta}_{\mathrm{d}\partial\delta}\times + \frac{1}{2}(\boldsymbol{\eta}_{\mathrm{d}\partial}\times\boldsymbol{\eta}_{\delta}\times + \boldsymbol{\eta}_{\partial\delta}\times\boldsymbol{\eta}_{\mathrm{d}}\times + \boldsymbol{\eta}_{\delta\mathrm{d}}\times\boldsymbol{\eta}_{\partial}\times + \boldsymbol{\eta}_{\mathrm{d}}\times\boldsymbol{\eta}_{\partial\delta}\times + \boldsymbol{\eta}_{\partial}\times\boldsymbol{\eta}_{\delta\mathrm{d}}\times + \boldsymbol{\eta}_{\delta}\times\boldsymbol{\eta}_{\mathrm{d}\partial}\times),
\end{aligned} \tag{B.13}$$

the associated differential maps of the exponential map of the rototranslation are obtained in either the direct form

$$\begin{aligned}
&\boldsymbol{\eta}_{\delta} = \boldsymbol{\Lambda}\delta\boldsymbol{\eta},\\
&\boldsymbol{\eta}_{\partial\delta} = \boldsymbol{\Lambda}\partial\delta\boldsymbol{\eta} + \boldsymbol{\Lambda}^{1\underline{2}\underline{3}}_{\mathrm{III}} : \partial\boldsymbol{\eta}\otimes\delta\boldsymbol{\eta},\\
&\boldsymbol{\eta}_{\mathrm{d}\partial\delta} = \boldsymbol{\Lambda}\mathrm{d}\partial\delta\boldsymbol{\eta} + \boldsymbol{\Lambda}^{1\underline{2}\underline{3}}_{\mathrm{III}} : (\mathrm{d}\boldsymbol{\eta}\otimes\partial\delta\boldsymbol{\eta} + \partial\boldsymbol{\eta}\otimes\delta\mathrm{d}\boldsymbol{\eta} + \delta\boldsymbol{\eta}\otimes\mathrm{d}\partial\boldsymbol{\eta})\\
&\qquad + \left(\boldsymbol{\Lambda}^{1\underline{\underline{2}}\underline{\underline{3}}\underline{\underline{4}}}_{\mathrm{IV}} - \left(\frac{1}{2}(\boldsymbol{I}^{\mathrm{x}}\boldsymbol{\Lambda})^{\mathrm{T}132}\boldsymbol{\Lambda}^{1\underline{2}\underline{3}}_{\mathrm{III}} + \boldsymbol{\Lambda}\otimes\boldsymbol{\Lambda}^{\mathrm{T}}\boldsymbol{\Lambda}\right)^{\mathrm{S}1\underline{\underline{2}}\underline{\underline{3}}\underline{\underline{4}}}\right) \vdots\ \mathrm{d}\boldsymbol{\eta}\otimes\partial\boldsymbol{\eta}\otimes\delta\boldsymbol{\eta},
\end{aligned} \tag{B.14}$$

and the inverse form

$$\begin{aligned}
&\delta\boldsymbol{\eta} = \boldsymbol{\Lambda}^{-1}\boldsymbol{\eta}_{\delta},\\
&\partial\delta\boldsymbol{\eta} = \boldsymbol{\Lambda}^{-1}\boldsymbol{\eta}_{\partial\delta} - \boldsymbol{\Lambda}^{-1\underline{2}\underline{3}}_{\mathrm{III}} : \boldsymbol{\eta}_{\partial}\otimes\boldsymbol{\eta}_{\delta},\\
&\mathrm{d}\partial\delta\boldsymbol{\eta} = \boldsymbol{\Lambda}^{-1}\boldsymbol{\eta}_{\mathrm{d}\partial\delta} - \boldsymbol{\Lambda}^{-1\underline{2}\underline{3}}_{\mathrm{III}} : (\boldsymbol{\eta}_{\mathrm{d}}\otimes\boldsymbol{\eta}_{\partial\delta} + \boldsymbol{\eta}_{\partial}\otimes\boldsymbol{\eta}_{\delta\mathrm{d}} + \boldsymbol{\eta}_{\delta}\otimes\boldsymbol{\eta}_{\mathrm{d}\partial})\\
&\qquad - \left(\boldsymbol{\Lambda}^{-1\underline{\underline{2}}\underline{\underline{3}}\underline{\underline{4}}}_{\mathrm{IV}} - \left(3\boldsymbol{\Lambda}^{-1\underline{2}\underline{3}}_{\mathrm{III}}\boldsymbol{\Lambda}\boldsymbol{\Lambda}^{-1\underline{2}\underline{3}}_{\mathrm{III}} - \frac{1}{2}\boldsymbol{\Lambda}^{-1}\boldsymbol{I}^{\mathrm{x}}\boldsymbol{\Lambda}\boldsymbol{\Lambda}^{-1\underline{2}\underline{3}}_{\mathrm{III}} + \boldsymbol{\Lambda}^{-1}\otimes\boldsymbol{I}\right)^{\mathrm{S}1\underline{\underline{2}}\underline{\underline{3}}\underline{\underline{4}}}\right) \vdots\ \boldsymbol{\eta}_{\mathrm{d}}\otimes\boldsymbol{\eta}_{\partial}\otimes\boldsymbol{\eta}_{\delta}.
\end{aligned} \tag{B.15}$$

The mapping tensors in Eqs. (B.14) come from the first dual nesting tensor and the relevant first and second derivatives,

$$\begin{aligned}
&\boldsymbol{\Lambda} = \boldsymbol{H}_{1},\\
&\boldsymbol{\Lambda}^{1\underline{2}\underline{3}}_{\mathrm{III}} = \boldsymbol{H}^{\mathrm{S}1\underline{2}\underline{3}}_{1/},\\
&\boldsymbol{\Lambda}^{1\underline{\underline{2}}\underline{\underline{3}}\underline{\underline{4}}}_{\mathrm{IV}} = \boldsymbol{H}^{1\underline{2}\underline{3}4\mathrm{S}1\underline{\underline{2}}\underline{\underline{3}}\underline{\underline{4}}}_{1//}.
\end{aligned} \tag{B.16}$$

The inverse form $\boldsymbol{\Lambda}^{-1}$, $\boldsymbol{\Lambda}^{-1\underline{2}\underline{3}}_{\mathrm{III}}$, $\boldsymbol{\Lambda}^{-1\underline{\underline{2}}\underline{\underline{3}}\underline{\underline{4}}}_{\mathrm{IV}}$ of the mapping tensors in Eqs. (B.15) are tied with the direct forms by the reciprocity relations

$$\begin{aligned}
&\boldsymbol{\Lambda}^{-1\underline{2}\underline{3}}_{\mathrm{III}} = \boldsymbol{\Lambda}^{-1}(\boldsymbol{\Lambda}^{1\underline{2}\underline{3}}_{\mathrm{III}}\boldsymbol{\Lambda}^{-1})^{\mathrm{T}132}\boldsymbol{\Lambda}^{-1},\\
&\boldsymbol{\Lambda}^{1\underline{2}\underline{3}}_{\mathrm{III}} = \boldsymbol{\Lambda}(\boldsymbol{\Lambda}^{-1\underline{2}\underline{3}}_{\mathrm{III}}\boldsymbol{\Lambda})^{\mathrm{T}132}\boldsymbol{\Lambda},\\
&\boldsymbol{\Lambda}^{-1\underline{\underline{2}}\underline{\underline{3}}\underline{\underline{4}}}_{\mathrm{IV}} = \boldsymbol{\Lambda}^{-1}((\boldsymbol{\Lambda}^{1\underline{\underline{2}}\underline{\underline{3}}\underline{\underline{4}}}_{\mathrm{IV}}\boldsymbol{\Lambda}^{-1})^{\mathrm{T}1423}\boldsymbol{\Lambda}^{-1})^{\mathrm{T}1423}\boldsymbol{\Lambda}^{-1},\\
&\boldsymbol{\Lambda}^{1\underline{\underline{2}}\underline{\underline{3}}\underline{\underline{4}}}_{\mathrm{IV}} = \boldsymbol{\Lambda}((\boldsymbol{\Lambda}^{-1\underline{\underline{2}}\underline{\underline{3}}\underline{\underline{4}}}_{\mathrm{IV}}\boldsymbol{\Lambda})^{\mathrm{T}1423}\boldsymbol{\Lambda})^{\mathrm{T}1423}\boldsymbol{\Lambda}.
\end{aligned} \tag{B.17}$$

B.4. Derivatives of the rototranslation exponential and tangent maps

The derivatives of the exponential and tangent maps of the rototranslation, namely tensors $\boldsymbol{H} \equiv \boldsymbol{H}_0$ and $\boldsymbol{\Lambda} \equiv \boldsymbol{H}_1$, are also given. From the differentiation formulae

$$\begin{aligned} \delta\boldsymbol{H} &= \boldsymbol{H}_{/} : \delta\boldsymbol{\eta} \otimes \boldsymbol{I}, \\ \delta\boldsymbol{\Lambda} &= \boldsymbol{\Lambda}_{/} : \delta\boldsymbol{\eta} \otimes \boldsymbol{I}, \end{aligned} \tag{B.18}$$

they become identified as the third-order dual tensors

$$\begin{aligned} \boldsymbol{H}_{/} &\equiv \boldsymbol{H}_{0/} = (\boldsymbol{H}\boldsymbol{I}^{\times}\boldsymbol{\Lambda}^{\mathrm{T}})^{\mathrm{T}132}, \\ \boldsymbol{\Lambda}_{/} &\equiv \boldsymbol{H}_{1/} = \boldsymbol{\Lambda}_{\mathrm{III}}^{\underline{12}\underline{3}} + \frac{1}{2}(\boldsymbol{I}^{\times}\boldsymbol{\Lambda})^{\mathrm{T}132}\boldsymbol{\Lambda}. \end{aligned} \tag{B.19}$$

We also give the explicit forms for such derivative dual tensors,

$$\begin{aligned} \boldsymbol{H}_{/} &= \boldsymbol{\Phi}_{/} + \varepsilon\,\boldsymbol{\Phi}_{//}^{\underline{12}\underline{34}} : \boldsymbol{\rho} \otimes \boldsymbol{I} \equiv \boldsymbol{\Phi}_{0/} + \varepsilon\,\boldsymbol{\Phi}_{0//}^{\underline{12}\underline{34}} : \boldsymbol{\rho} \otimes \boldsymbol{I}, \\ \boldsymbol{\Lambda}_{/} &= \boldsymbol{\Gamma}_{/} + \varepsilon\,\boldsymbol{\Gamma}_{//}^{\underline{12}\underline{34}} : \boldsymbol{\rho} \otimes \boldsymbol{I} \equiv \boldsymbol{\Phi}_{1/} + \varepsilon\,\boldsymbol{\Phi}_{1//}^{\underline{12}\underline{34}} : \boldsymbol{\rho} \otimes \boldsymbol{I}, \end{aligned} \tag{B.20}$$

where $\boldsymbol{\Phi}_{/}$ and $\boldsymbol{\Gamma}_{/}$ are given by Eqs. (A.16). Again, the dual parts of Eqs. (B.20) are linear with vector $\boldsymbol{\rho}$ and should be compared with Eqs. (A.17).

B.5. The translation vector

We close Appendix B with a noteworthy characterization of the translation vector in terms of the single primal and dual parts of the helix. We know from Eqs. $(A.10)_1$ and $(A.15)_1$ that $\delta\boldsymbol{\Phi} = \boldsymbol{\varphi}_{\delta}\times\boldsymbol{\Phi} = \boldsymbol{\Phi}_{/} : \delta\boldsymbol{\varphi} \otimes \boldsymbol{I}$. Moreover, we know the form of a rototranslation tensor by means of the rotation tensor $\boldsymbol{\Phi}$ and the translation vector $\boldsymbol{t}$ (see Part I), so that, by recalling Eqs. (B.5) and $(A.16)_1$, we can write $\boldsymbol{H} = \boldsymbol{\Phi} + \varepsilon\,\boldsymbol{t}\times\boldsymbol{\Phi} = \boldsymbol{\Phi} + \varepsilon\boldsymbol{\Phi}_{/} : \boldsymbol{\rho} \otimes \boldsymbol{I}$. By comparing the dual part of the rototranslation $\boldsymbol{H}$ with $\delta\boldsymbol{\Phi}$, and recalling Eq. $(A.11)_1$, we arrive at the relation

$$\boldsymbol{t} = \boldsymbol{\Gamma}\boldsymbol{\rho}. \tag{B.21}$$

So, the translation vector is depending linearly on the dual part of the helix, and nonlinearly on the primal part. Eq. (B.21) maps the linear part of the helix onto the translation vector. It is worth noting that this map exploits the same mapping tensor as the tangent map of the rotation.

References

Angeles, J., 1998. The application of dual algebra to kinematic analysis. In: Angeles, J., Zakhariev, E. (Eds.), Computational Methods in Mechanical Systems, vol. 161. Springer-Verlag, Heidelberg, pp. 1–31.

Bauchau, O.A., Trainelli, L., 2003. The vectorial parametrization of rotation. Nonlinear Dyn. 32, 71–92.

Borri, M., Bottasso, C., 1994a. An intrinsic beam model based on a helicoidal approximation—Part I: Formulation. Int. J. Numer. Meth. Eng. 37, 2267–2289.

Borri, M., Bottasso, C., 1994b. An intrinsic beam model based on a helicoidal approximation—Part II: Linearization and finite element implementation. Int. J. Numer. Meth. Eng. 37, 2291–2309.

Borri, M., Bottasso, C.L., 1998. The exponential map of motion—theory and applications. In: Idelsohn, S.R., Oñate, E., Dvorkin, E. (Eds.), Computational Mechanics. New trends and applications. ©CIMNE, Barcelona, Spain.

Borri, M., Trainelli, L., Bottasso, C.L., 2000. On representations and parameterizations of motion. Multibody Syst. Dyn. 4, 129–193.

Cardona, A., Geradin, M., 1988. A beam finite element non-linear theory with finite rotations. Int. J. Numer. Meth. Eng. 26, 2403–2438.

Crisfield, M., Jelenić, G., 1999. Objectivity of strain measures in the geometrically exact three dimensional beam theory and its finite-element implementation. Proc. R. Soc. Lond. A 455, 1125–1147.

de Souza Neto, E.A., 2001. The exact derivative of the exponential of an unsymmetric tensor. Comput. Methods Appl. Mech. Eng. 190, 2377–2383.

Ibrahimbegović, A., Frey, F., Kožar, I., 1995. Computational aspects of vector-like parametrization of three-dimensional finite rotations. Int. J. Numer. Methods Eng. 38, 3653–3673.

Ibrahimbegović, A., Taylor, R.L., 2002. On the role of frame-invariance in structural mechanics models at finite rotations. Comput. Methods Appl. Mech. Eng. 191, 5159–5176.

Itskov, M., 2000. On the theory of fourth-order tensors and their applications in computational mechanics. Comput. Methods Appl. Mech. Eng. 189, 419–438.

Itskov, M., 2002. The derivative with respect to a tensor: some theoretical aspects and applications. ZAMM Z. Angew. Math. Mech. 82, 535–544.

Itskov, M., Aksel, N., 2002. A closed-form representation for the derivative of non-symmetric tensor power series. Int. J. Solids Struct. 39, 5963–5978.

Jelenić, G., Crisfield, M.A., 1999. Geometrically exact 3D beam theory: implementation of a strain-invariant finite element for statics and dynamics. Comput. Methods Appl. Mech. Eng. 171, 141–171.

Merlini, T., 2002. Differentiation of rotation and rototranslation. DIA-SR 02-16, Dip. Ing. Aerospaziale, Politecnico di Milano.

Merlini, T., 2003. Recursive representation of orthonormal tensors. DIA-SR 03-02, Dip. Ing. Aerospaziale, Politecnico di Milano.

Merlini, T., Morandini, M., 2003. Interpolation of the orientation and oriento-position fields. DIA-SR 03-03, Dip. Ing. Aerospaziale, Politecnico di Milano.

Ortiz, M., Radovitzky, R.A., Repetto, E.A., 2001. The computation of the exponential and logarithmic mappings and their first and second linearizations. Int. J. Numer. Meth. Eng. 52, 1431–1441.

Ring, M.C., 2003. MAPM Version 4.8 (Mike's Arbitrary Precision Math Library). Available from <http://www.tc.umn.edu/~ringx004/mapm-main.html>.

Ritto-Corrêa, M., Camotim, D., 2002. On the differentiation of the Rodrigues formula and its significance for the vector-like parameterization of Reissner–Simo beam theory. Int. J. Numer. Methods Eng. 55, 1005–1032.

Rosati, L., 1999. Derivatives and rates of the stretch and rotation tensors. J. Elast. 56, 213–230.